Engineering Molecular Ligand Shells on Quantum Dots for Quantitative Harvesting of Triplet Excitons Generated by Singlet Fission

Jesse R. Allardice[a], Arya Thampi[a], Simon Dowland[a], James Xiao[a], Victor Gray[a,d], Zhilong Zhang[a], Peter Budden[a], Anthony J. Petty II[b], Nathaniel J. L. K. Davis[c,a], Neil C. Greenham[a], John E. Anthony[b] and Akshay Rao[a]

Contacts

[a]Cavendish Laboratory, University of Cambridge, J. J. Thomson Avenue, Cambridge, CB3 0HE, UK

[b]Center for Applied Energy Research, University of Kentucky, Research Park Dr., Lexington KY 40511, USA

[c]The MacDiarmid Institute for Advanced Materials and Nanotechnology, The Dodd-Walls Centre for Photonic and Quantum Technologies, School of Chemical and Physical Sciences, Victoria University of Wellington, Wellington 6140, New Zealand.

[d]Department of Chemistry, Ångström Laboratory, Uppsala University, Box 532, SE-751 20 Uppsala, Sweden

Abstract

Singlet fission is an exciton multiplication process in organic molecules, in which a photogenerated spin-singlet exciton is rapidly and efficiently converted to two spin-triplet excitons. This process offers a mechanism to break the Shockley–Queisser limit by overcoming the thermalisation losses inherent to all single junction photovoltaics. One of the most promising methods to harness the singlet fission process is via the efficient extraction of the dark triplet excitons into Quantum Dots (QDs) where they can recombine radiatively, thereby converting high-energy photons to pairs of low energy photons, which can then be captured in traditional inorganic PVs such as Si. Such a singlet fission photon multiplication (SF-PM) process could increase the efficiency of the best Si cells from 26.7% to 32.5%, breaking the Shockley–Queisser limit. However, there has been no demonstration of such a singlet fission photon multiplication (SF-PM) process in a bulk system to date. Here, we demonstrate a solution-based bulk SF-PM system, based on the singlet fission material TIPS-Tc combined with PbS QDs. Using a range of steady-state and time-resolved measurements, combined with analytical modelling we study the dynamics and mechanism of the triplet harvesting process. We show that the system absorbs >95% of incident photons within the singlet fission material to form singlet excitons, which then undergo efficient singlet fission in the solution phase (135±5%) before quantitative harvesting of the triplet excitons (95±5%) via a low concentration of QD acceptors, followed by the emission of IR photons. We find that in order to achieve efficient triplet harvesting it is critical to engineer the surface of the QD with a triplet transfer ligand and that bi-molecular decay of triplets is potentially a major loss pathway which can be controlled via tuning the concentration of QD acceptors. We demonstrate that the photon multiplication efficiency is maintained up to solar fluence. Our results establish the solution-based SF-PM system as a simple and highly tuneable platform to understand the dynamics of triplet energy transfer process between organic semiconductors and QDs, one that can provide clear design rules for new materials.

Introduction

The quest to increase the efficiency of solar energy harvesting has been a major scientific challenge since the invention of the photovoltaic cell (PV).[1] Single junction cells made from semiconductors such as silicon and GaAs have been well optimised and attain very high efficiencies of 26.7% and 29.1% respectively.[2,3] However, the efficiency of all single junction cells is fundamentally capped by the Shockley–Queisser limit.[4] There is thus a need to develop technologies that can overcome these fundamental limits to the efficiency of singlet junction cells.

Singlet fission is an exciton multiplication process occuring in a variety of organic semiconductor materials.[5,6] Here, one photogenerated spin-0 singlet exciton is converted to two spin-1 triplet excitons via a spin-allowed mechanism. Shortly after the discovery of the singlet exciton fission process (1968),[7–10] it was proposed as a route to break the Shockley–Queisser limit (1979) by reducing the energy lost by thermalisation of photoexcited charge carriers with excess energy above the bandgap.[11] However, while there has been a larger effort in recent years to develop new singlet fission molecules and understand the fundamental photo physics of the process, there have been only been a few studies of how to harvest the triplet excitons generated via fission to improve the efficiency of inorganic PV cells, such as Si cells.[12–15]

One of the most promising methods to harness fission is to harvest the energy of the fission generated triplets via luminescence.[16] In such a scheme, each high energy photon absorbed by the singlet fission materials would lead to the formation of two triplet excitons via fission which would then be converted to two low energy photons, to be absorbed by a conventional inorganic PV cells, thus doubling the photocurrent from the high energy part of the solar spectrum. This scheme, termed a singlet fission photon multiplier (SF-PM), has been described recently and its potential effect on cell efficiencies calculated.[17] It was shown that it could increase the efficiency of the best Si PV cells available today from 26.7% to 32.5%, thus breaking through the Shockley–Queisser limit for the silicon bandgap. The SF-PM is also technologically attractive as it does not require modification of the underlaying inorganic PV, but rather can be coated on top of it.

Since triplet excitons are dark states, due to their spin-forbidden return to the ground state, they cannot directly emit photons.[5] Hence, a key breakthrough was the demonstration of transfer of triplet excitons to colloidal inorganic quantum dots (QDs), where the excitations become bright and can recombine to emit photons.[18,19] This discovery also led to the study of the reverse process, the transfer of energy from QDs to the triplet state of organic semiconductors, for application in upconversion and triplet sensitisation to drive photochemical reactions.[20,21] Numerous studies in this area have focused on the role of the ligand on the QD in facilitating or hindering transfer of energy to the organic semiconductor.[22–24] These ligands both passivate surface defects and provide the QDs with colloidal stability. The transfer dependence on the length of the ligands indicated a Dexter-like transfer mechanism, with shorter ligands providing more efficient transfer as the ligands serve as a tunnel barrier.[25,26] However, for the transfer of triplets into QDs, the basis of current SF-PM

technologies, there have been no equivalent studies looking at triplet harvesting in bulk systems. The two previous reports of triplet transfer to QDs, considered bilayer systems containing layers of organic and QDs on top of each other. [18,19] The confined and bilayer nature of the system means that triplets formed via fission are always close to an interface with the QDs and hence have ample opportunity to tunnel across the ligands. However, such a scheme does not provide sufficient light absorption as to be of any practical use. In a useful SF-PM, the singlet fission material must be present in sufficient quantity to harvest most of the incident photons (>95%) and at the same time the QDs must be present in a low concentration so as to minimise parasitic loss via absorption of solar photons by QDs (<5%).[17] No such bulk system has yet been demonstrated, and the dynamics of the triplet transfer process to the QDs in such system remain unexplored.

Here, we report a solution-based bulk SF-PM system in which >95% of incident photons are absorbed by the singlet fission material. Efficient singlet fission then occurs in the solution phase (135±5%) before the triplet excitons are quantitatively (95±5%) harvested via a low concentration of QDs (<50 mg/mL)), followed by the emission of IR photons. Our solution phase SF-PM consists of a blend of a highly soluble singlet fission material, 5,12-bis-((triisopropylsilyl)ethynyl)tetracene) referred to as TIPS-Tc,[27] and lead sulphide (PbS) QDs covered in 6,11-bis-((triisopropylsilyl)ethynyl)tetracene-2-carboxylic acid)) ligands, referred to as TetCAL, together in toluene solution. The TIPS-Tc absorbs photons via its $S_0 \rightarrow S_1$ transition (2.32 eV), while the triplets generated by singlet fission are efficiently transferred to the PbS QDs via the TetCAL ligands, resulting in IR luminesce (Figure 1b). Using a range of steady-state and time-resolved measurements, combined with analytical modelling we study the dynamics and mechanism of the triplet harvesting process and show that in order to achieve efficient triplet harvesting it is critical to engineer the surface of the QD with a triplet transfer ligand, TetCAL, analogous to recent work with QD-organic based up-conversion systems.[23] Our results demonstrate that under solar-equivalent fluences it is possible to efficiently harvest triplet excitons in a bulk system via a low concentration of QDs, with sufficiently low QD parasitic absorption for realistic coupling to a Si PV cell and establishes design rules for such a process.[17] Our solution-based system also serves as a simple and highly tuneable platform to understand the dynamics of triplet energy transfer process between organic semiconductors and QDs.

Results and Discussion

Characterisation of TIPS-Tc + PbS/TetCAL Solution SF-PM System. The synthesis of PbS QDs with oleic acid ligands (OA) and subsequent ligand exchange with either TetCAL or hexanoic acid (HA) was carried out using an adaptation of previously reported methods.[28] Figure 1c shows the absorption and emission spectra of TIPS-Tc, TetCAL, PbS QDs with the native OA ligands (PbS/OA) and those modified with TetCAL via ligand exchange (PbS/TetCAL). Attachment of the TetCAL ligand after multiple wash cycles in acetone is confirmed via UV-Vis absorption measurements, where the TetCAL absorbance peaks are visible on top of the PbS QD absorbance. The absorption of TIPS-Tc, TetCAL and PbS/TetCAL show clear vibrionic structure. The 0-0 vibrionic peak of TIPS-Tc at 535 nm

gives an S_1 energy of 2.32 eV, while the TetCAL 0-0 peak at 545 nm (2.28 eV) indicates a 40 meV red shift on addition of the carboxylic acid functional group. The triplet energy of TIPS-Tc is expected to be 1.2 eV,[27] meaning that singlet fission in TIPS-Tc is endothermic.

The PbS QDs are tuned such that their bandgap, as measured from the excitonic absorption peak at ~1180 nm (~ 1.05 eV), is below the triplet energy of TIPS-Tc (~ 1.2 eV), making it energetically favourable to accept triplets from TIPS-Tc.[18] The Stokes-shifted PbS QD photoluminescence peak is at ~1350 nm (~ 0.92 eV). TIPS-Tc is a well-studied singlet fission material, which has been shown to efficiently undergo fission in high-concentration solutions (>200 mg/mL) with a fission yield of 120 ± 10%.[27,29]

TetCAL is designed to act as a triplet transmitter ligand, whose triplet energy will lie above the bandgap of the QDs and slightly below that of the TIPS-Tc fission material, due to the conjugation of the COOH group which slightly lowers the energy levels in comparison to TIPS-Tc. As illustrated in Figure 1a, transfer of a triplet between TIPS-Tc and the PbS/OA QD would have to occur over a large distance. The oleic acid ligands act as a tunnelling barrier, resulting in a large Dexter transfer distance and thus reducing the rate of transfer.[18,19] Whereas, with the TetCAL ligand acting as a transmitter, the triplet exciton can first transfer to the ligand. After this initial triplet transfer, the Dexter transfer distance into the PbS QD has been significantly decreased compared to transfer through either OA or HA.[23]

Molar absorption coefficients for the various species were measured across the Vis-NIR range. In particular the molar attenuation coefficients at 515 nm for TIPS-Tc, PbS/OA and PbS/TetCAL were found to be 2.4×10^4, 2.6×10^5, and 3.5×10^5 $Lmol^{-1}cm^{-1}$, respectively (Figure S2). These attenuation coefficients have been used to calculate the relative absorption of photons in each species for varying concentration of the blends components. The measured absorbance of a 15 µm thick solution of TIPS-Tc and PbS/TetCAL QDs shows the TIPS-Tc absorbance peak (535 nm) is two orders of magnitude higher than the parasitic absorbance of the PbS QD (Figure S4a). Using the molar attenuation coefficients for the solution PM the absorption for a 2.5 µm thick solution is predicted to be >95% at the TIPS-Tc peak while the QD parasitic absorption will be less than 5%, thus fulfilling the absorption criteria for a "realistic" SF-PM proposed previously (Figure S4c,d).[17]

We perform qualitative evaluation of the SF-PM system by measuring IR-detected photoluminescence excitation spectra. Figure 2a shows the photoluminescence (PL) excitation scan of a solution of PbS/OA QDs in toluene (50 mg/mL), along with the comparable excitation scans for blends of TIPS-Tc (200 mg/mL) and QDs with various ligands, normalised to the value at 700 nm excitation.[18] The excitation scan of PbS/OA has a decreasing emission with increasing wavelength, following the absorbance of the QDs across this region. At wavelengths above 600 nm, where only the QDs are absorbing, all solutions follow the same trend. However, at wavelengths less than this the concentrated TIPS-Tc, with orders of magnitude higher absorption, is absorbing most of the light (Figure S4) and so the IR PL from the solution is an indication of the amount of exciton transfer from TIPS-Tc to the QDs. Compared to PbS/OA on its own, TIPS-Tc + PbS/TetCAL solution, show an increase in the IR PL for wavelengths where the TIPS-Tc is absorbing, with the PL excitation peaks matching

with TIPS-Tc absorption peaks, indicating a high exciton transfer efficiency. In contrast blends of TIPS-Tc and PbS QDs without the TetCAL ligand (either OA or HA ligands) show a significant drop in IR PL for excitation below 550 nm, with dips that match with the absorption peaks of TIPS-Tc. This shows that for these solutions energy transfer from TIPS-Tc to the QDs is inefficient.

For quantitative evaluation of the SF-PM system we use IR PLQE measurements on a series of solutions with varying QD concentrations. By comparing the IR PLQE values when the solution is excited at 515 nm, which excites both TIPS-Tc and QD, or at 658 nm, which selectively excites the QDs, the efficiency of exciton transfer can be determined (Figure 2b). For TIPS-Tc + PbS/TetCAL solutions the peak PLQE occurs at a QD concentration of 50 mg/mL, with 18.2% IR PLQE (515 nm excitation), while the intrinsic PLQE of the QD in the same solution was found to be 14.6% (658 nm excitation) (Table S1).

The IR PLQE of a photon multiplier, $\eta_{PM}(\lambda)$, for excitation at wavelength λ, with singlet fission donor and emissive QD acceptor components, can be expressed as,[18]

$$\eta_{PM}(\lambda) = \eta_{QD}\frac{\mu_{QD}(\lambda)+\eta_{Tr}\mu_{Tc}(\lambda)}{\mu_{QD}(\lambda)+\mu_{Tc}(\lambda)}. \qquad (1)$$

Where η_{QD} is the intrinsic PLQE of the QD, μ_i is the attenuation coefficient, base 10, of the ith component and η_{Tr} is the total exciton transfer efficiency from the donor to acceptor. Using equation (1), the measured molar absorption coefficients and the intrinsic QD PLQEs, we calculate the exciton transfer efficiency, η_{Tr}, as shown in Figure 2b (see supplementary section 4 for details). Here, we have quantitative proof of singlet fission photon multiplication, as we observe values of exciton transfer above 100%, for concentrations greater than ~10 mg/mL of PbS/TetCAL QDs. Magnetic field dependent PL measurements confirm that we are harvesting triplet excitons generated via singlet fission (Figure S31).[18]

The PLQE and transfer efficiency values for 100 mg/mL QD concentration have been highlighted as outliers due to self-absorption losses (Figure 2b). Self-absorption is identified from the drop in intrinsic PLQE and red shifting of the PL spectrum (Figure S6). The measured transfer efficiencies, η_{Tr}, for the PbS/OA system are low for all QD concentrations, indicating poor exciton transfer. Changing the QD ligand to HA does result in slightly increased IR PL when the TIPS-Tc is absorbing. This trend agrees with the HA ligand resulting in higher exciton transfer than the longer OA ligand due to HA having a shorter Dexter transfer distance.[18,19,25] However, the TetCAL ligand greatly outperforms the shorter HA ligands.

Along with the increased steady state PLQE we measure a longer lived transient PL signal for PbS/TetCAL+ TIPS-Tc compared to PbS/OA+ TIPS-Tc, when excited at 530 nm, as shown in Figure. 2c. This indicates that the triplet exciton transfer is occurring on time scales comparable to or slower than the decay of the excited QD states. Due to the long lifetime of the QDs compared to the fixed repetition rate (1 MHz) used to photo-excite the system, a significant population of excited TIPS-Tc and QD states, were still present when the next pump laser pulse interacts with the system. This effect is most apparent by the high PL counts before time zero. This represents real photon counts from the sample, as the electronic noise that contributes a background has been removed

(supplementary section 7). We use a bi-exponential decay in the presence of a periodic excitation to fit the decay of the QD PL (supplementary section 7). The short time constant component is a parameterisation of the non-linear recombination occurring in the QD, while the longer time constant is the decay constant for excited QD states. When the SF-PM solutions are excited at 530 nm, where TIPS-Tc's absorption is dominant, we extract a decay constant of 1.30±0.01 μs for the PbS/OA quantum dots, compared to 22.0 ±0.7 μs for the PbS/TetCAL QDs. The value for PbS/OA QDs is in agreement with previous reports for PbS/OA QDs alone in toluene, however the PbS/TetCAL value is significantly longer.[22] This suggests the TIPS-Tc triplet excited states are feeding the PbS/TetCAL QDs (10 mg/mL) with a time constant of around 20 μs.

Investigation of TIPS-Tc Singlet Fission by Femtosecond Transient Absorption. To evaluate the ultrafast excited-sate dynamics of TIPS-Tc in the presence of PbS QDs, femtosecond transient absorption spectra were measured (Figure S10,11). In concentrated solutions of TIPS-Tc (200 mg/mL), with and without PbS/TetCAL (50 mg/mL), we observe a loss of the singlet and rise of triplet features within 100 ps after excitation (supplementary section 8).[27,29] Comparing the decay of the singlet exciton in both cases reveals no significant difference in the fission kinetics and shows that singlet exciton transfer to the QD cannot compete with the singlet fission rate. We put an upper bound on singlet exciton transfer efficiency from the initially excited TIPS-Tc singlet to the PbS/TetCAL QDs at 5% (supplementary section 8). We see no significant growth of QD features in the first 2 ns after photo excitation. Therefore, the transfer being observed is predominantly triplet transfer on timescale greater than 2 ns.

Investigation of Triplet Transfer by Nanosecond Transient Absorption. To investigate the full decay of the excited states in TIPS-Tc and PbS/TetCAL, nanosecond transient absorption (nsTA) spectra were measured, as shown in Figure 3a. After fs pulse excitation at 535 nm, we observe initial nsTA spectra that contain both TIPS-Tc triplet and excited state QD features in the NIR probe region (750-1250 nm). We identify the TIPS-Tc triplet excitons by the two photoinduced absorption (PIA) peaks at 840-850 and 960-970 nm.[27,29] The positive signal at 950-1200 nm is assigned to a ground state bleach (GSB) from QD excited states.[19]

In solutions of concentrated pristine TIPS-Tc we observe long-lived (>10 μs) triplet excitons as identified by the triplet PIA features (Figure S12), which is consistent with previous literature.[27] Additionally, we identify a broad PIA feature across the probe range, identified as an excimer state, decaying within 10 ns.[27,29] The decay of TIPS-Tc triplets display significant fluence dependence, indicating bi-molecular recombination as a significant decay channel for the excited triplet states (Figure S12). Global fitting of multiple nsTA kinetics (at varying laser fluences), following previously reported methods for fitting triplet decay dynamics, involving an analytic model for a second order rate equation, allows extraction of the monomolecular and bi-molecular triplet decay rates of 5.6 ± 5.1 $(ms)^{-1}$ and $(7.6 \pm 0.3) \times 10^{-23} \mathrm{cm}^3 \mathrm{ns}^{-1}$, respectively (Table S5).[30] The significant uncertainty on the mono-molecular decay rate indicates that we have not fully resolved the intrinsic decay of the triplet states. Given the uncertainty in the extracted values, comparison of the decay rate shows at most 40% of triplets decay mono-molecularly at the lowest laser fluence used, 21 $\mu J/cm^2$, the rest decaying via bi-molecular channels.

In the presence of either PbS/OA or PbS/TetCAL we observe no effect on the generation of triplets via singlet fission in TIPS-Tc, evident by the similar initial nsTA intensity of the triplet PIA features (Figure S16). For both QDs types, at early times the negative nsTA feature corresponding to the TIPS-Tc excimer PIA, overlaps with the GSB and PIA of the QDs. The decay of this negative feature, produces an apparent rise in the positive ground state QD GSB signals which overlap in the 1140-1160 nm region. This rise in signal is thus not associated with a change in QD population (Figure 3b). At 10 ns, the PbS/OA and PbS/TetCAL GSB signals are of similar intensities, indicating similar initial populations of excited QDs in both systems. We assign this initial TA signal to the fraction of photons that directly excite the QDs with the 535 nm pump pulse. After the initial direct excitation of the PbS/OA QDs we observe a decay in the excited QD signal characterised by a 1.8 ± 0.1 µs decay constant. In comparison the solution with PbS/TetCAL QDs (100 mg/mL) shows a significantly longer 5.1 ± 0.2 µs decay constant for the QDs. This is longer than its intrinsic 1.90 ± 0.05 µs lifetime (Figure S13). This increased time constant is consistent with delayed triplet transfer to the QDs and is thus consistent with the TrPL data shown in Figure 2c.

To clarify the quenching of the TIPS-Tc triplets and transfer to the PbS/TetCAL QDs, difference nsTA maps were calculated. The nsTA spectra for PbS/TetCAL (under 535 nm excitation) was linearly scaled to match with the initial QD GSB (in the range 20-40 ns) in the TIPS-Tc+PbS/TetCAL blends and the difference was calculated.[31] The difference nsTA maps contain information about excited QDs resulting from transfer, without contribution from directly excited PbS/TetCAL QDs (Figure 3c and S18). After this transformation the loss of the TIPS-Tc triplets corresponding with a rise in the QD GSB is clear. The strength of the QD GSB that grows in after 100 ns, is seen to increase with the concentration of the QDs (Figure S19), consistent with diffusion-limited transfer. Applying linear regression of the pristine TIPS-Tc triplet spectrum to the difference maps allows extraction of the magnitude of the TIPS-Tc triplet PIA spectrum as a function of time and QD concentration, as seen in Figure 3d (details in section S8). Comparing these triplet PIA lifetimes shows a quenching that is dependent on PbS/TetCAL QD concentration.

Kinetic Model: We use the following kinetic model to describe the transfer of triplets from the TIPS-Tc to the PbS/TetCAL QDs,

$$\frac{dT_1}{dt} = -(k_T + k_{TET}X_0)T_1 - k_2T_1^2, \qquad (2)$$

$$\frac{dX_1}{dt} = k_{TET}X_0T_1 - k_XX_1, \qquad (3)$$

where T_1 is the triplet density produced via singlet fission with an efficiency η_{SF}, X_1 is the density of excited QD states, k_T and k_2 are the intrinsic and bi-molecular decay rate constants for TIPS-Tc triplets, k_{TET} is the triplet transfer rate to the PbS/TetCAL QDs, k_X is the QD decay rate and X_0 is the concentration of the QD acceptor. Using the bimolecular triplet decay rate obtained for pristine TIPS-Tc as a fixed input parameter, we apply fitting of analytical solution for the 2nd order rate equation and extract the mono-molecular decay rate as a function of PbS/TetCAL QD concentration, $k_1 = k_T + k_{TET}X_0$ (inset, Figure 3d). Applying this Stern-Volmer like quenching model we extract a triplet transfer rate of k_{TET} = 0.0039 ± 0.0001 $(mg/mL)^{-1}\mu s^{-1}$ (5.1x10^8 ± 0.1x10^8 $M^{-1}s^{-1}$) and an intrinsic

triplet lifetime of τ_T = 250 ± 180 µs.[30] The reasonable agreement with a linear relation between TET rate and QD acceptor concentration indicates that the triplet transfer is diffusion-limited, not kinetically limited. Using triplet exciton diffusion constants from previously reported diffusion-ordered nuclear magnetic spectroscopy measurements and assuming relatively low diffusion of the PbS/TetCAL QD, we estimate the diffusion-limited transfer rate to be 0.085 ± 0.012 $(mg/mL)^{-1}\mu s^{-1}$ (supplementary section 6).[27] This is roughly a factor of 20 times higher than what we observe. Possible reasons for this disagreement include, a low Gibbs free energy to drive the transfer, non-uniform coverage of the TetCAL ligand over the surface of the PbS/TetCAL QDs and steric hindrance from residual OA ligands attached to the QD.[32]

Using the extracted intrinsic PbS/TetCAL QD lifetime and triplet transfer rate, the simulated dynamics for the decay of the triplet excitons and the excited state QDs are calculated and shown in Figure 3c along with the TIPS-Tc triplet difference PIA signal and the QD GSB signal (1140-1160 nm) (details in supplementary section 8). Agreement with the two species model described by equations 2 and 3 suggests that the transfer of triplet excitons from the TetCAL molecules into the QD is not rate limiting. However, this step should still be seen as critically important for the transfer process. Additionally, we calculate the triplet transfer efficiency, η_{TET}, as a function of the PbS/TetCAL QD concentration, at the laser fluence used in the IR PLQE measurements. Multiplication of this TET efficiency with a singlet fission yield of, $\eta_{SF} = 135 \pm 5\%$, gives reasonable agreement with the observed values for the exciton transfer efficiency, $\eta_{Tr} = \eta_{SF}\eta_{TET}$, from our PLQE data (Figure 2b, grey curve). This value for the singlet fission yield agrees with previous predictions obtained via the magnitude of transient absorption spectra.[27] For the 50 mg/mL solution of PbS/TetCAL QDs we calculate a triplet exciton transfer efficiency of $\eta_{TET} = 95 \pm 5\ \%$, approaching 100% at higher QD concentration (Figure S27).

Unexpectedly the nsTA data suggest that triplet exciton transfer in TIPS-Tc+PbS/TetCAL solutions is significantly hindered by bi-molecular decay of the TIPS-Tc triplets, presenting a concern for the versatility of this SF-PM to operate in real world conditions under solar irradiance.

Determining the Solution Phase SF-PM Fluence Dependence. To evaluate the effect of bi-molecular triplet decay on the photon multiplication efficiency of TIPS-Tc+PbS/TetCAL blends, steady state PL spectra were measured at a range of laser fluences, as shown in Figure 4a. Here we measure the PL from the QDs that arises after the fission and triplet transfer process. At lower excitation densities the QD IR PL increases linearly with the flux, but then passes through a threshold triplet generation density, G_{Th}, after which the QD PL goes as the square root of the excitation density. Modelling of the system (see supplementary section 10) reveals that the threshold triplet generation rate per unit volume, $G_{Th,}$ is given by,

$$G_{Th} = \frac{(k_T + k_{TET}X_0)^2}{k_2}. \quad (4)$$

Equation (4) shows that this threshold will increase with QD concentration. The data for TIPS-Tc with 2 mg/mL of PbS/TetCAL QDs show a change from linear to square-root dependence at a threshold

intensity of 2.9 ± 1.0 mW/cm^2, consistent with the value of 2.0 ± 1.2 mW/cm^2 expected from equation (4) and the nsTA kinetic parameters. In contrast, the solution with the higher concentration of QDs (100 mg/mL) shows little deviation from a linearity over the range of intensities studied, indicating an insignificant effect from the bi-molecular decay of triplets. The PLQE is therefore maintained up to equivalent solar fluences (the photon flux available for absorption by TIPS-Tc under the AM1.5G spectrum) (Figure S30 and supplementary section 11). This shows that the TIPS-Tc + PbS/TetCAL solutions are appropriate to use as a SF-PM under practical conditions.

Figure 4b shows simulations of the normalised photon multiplication efficiency, η_{PM}/η_{QD}, across a range of power flux and PbS/TetCAL QD concentrations. The results reveal that the intrinsic QD PLQE can be exceeded for a wide range of configurations. However, if we aim for a higher value of η_{PM}/η_{QD} equal to 0.95η_{SF} (corresponding to 95% of the initial singlet fission efficiency) this significantly reduces the useful parameter space, as shown by the highlighted contour in Figure 4b, where the dotted red line corresponds to solar fluence. Thus, a minimum concentration of 30-40 mg/mL of QDs is required to efficiently harvest the bulk of the triplets generated at solar fluence for this system. As we have shown, this is limited by the bimolecular triplet-triplet recombination of TIPS-Tc.

Conclusion

We have demonstrated a solution-based bulk SF-PM system, in which >95% of incident photons are absorbed by the singlet fission material, TIPS-Tc. Efficient singlet fission occurs in the solution phase before quantitative harvesting of the triplet excitons via a low concentration of PbS QDs (≤ 50 mg/mL)), followed by the emission of IR photons. We have shown that in order to obtain efficient harvesting of the fission generated triplets it is necessary to engineer the surface ligands on the PbS QDs. TetCAL ligands are shown to be much more efficient that either OA or HA. Several surprising results are uncovered; for instance while the transport of the TIPS-Tc triplets to the PbS/TetCAL QD is the rate-limiting step, it occurs more slowly than would be expected for a purely diffusion limited process suggesting that there exists a mixed nature of the QD ligand coverage (consisting of both of the TetCAL and OA). This leads to the need for multiple collisions before transfer is achieved to the TetCAL ligand. We also find that bi-molecular recombination of triplets is the major loss channel and limits the photon multiplication performance at high fluences. However, it is possible to arrange a sufficiently high concentration of QDs (30-50 mg/mL) such that 95% of the triplets present can be harvested at solar fluence, but still minimise parasitic absorption such that at energies below the absorption of TIPS-Tc less than 5% of photons are absorbed by the PbS QDs. These results thus establish that it is possible to have a photon multiplication scheme that can function at solar fluence and shows the potential of singlet fission photon multiplication as a means to break the Shockley–Queisser limit. Currently the limiting performance factors are the PLQE of the PbS/TetCAL quantum dots and the TIPS-Tc singlet fission yield. With the current singlet fission yield of 135%, a QD with

PLQE larger than 80% would be required in order to achieve an overall photon multiplication yield greater than 100%.

Future improvements to the photon multiplication scheme should focus on increasing the transfer rate, resulting in a larger parameter space where triplets are effectively extracted with the need for lower concentration of QDs (Figure S29). A reduction in the rate of bi-molecular recombination of triplets would also be highly desirable, for instance by tuning electronic structure such that TTA events lead solely to the reformation of the singlet state, which could then be recycled. Lessons can be learnt from the photon upconversion field, where TTA yields for singlet generation can approach 100%.[30] Ultimately, the SF-PM will require solid-state implementation, which will require careful control of nano-morphology, as well as energetics and surface chemistry of the QDs. The solution-based SF-PM system we have established here serves as a convenient and highly tuneable platform to understand the fundamental photophysics of the triplet transfer process from organic semiconductors to QDs, and to test materials combination, energetics and surface chemistries, in order to guide the future development of solid-state SF-PM systems.

Acknowledgments:

The authors thank the Winton Programme for the Physics of Sustainability and the Engineering and Physical Sciences Research Council for funding. J. R. A. acknowledges Cambridge Commonwealth European and International Trust for financial support. J. X. acknowledges EPSRC Cambridge NanoDTC, EP/L015978/1 for financial support. JEA and AJP acknowledge the U.S. National Science Foundation (DMREF-1627428) for support of organic semiconductor synthesis. V.G. acknowledges funding from the Swedish Research Council, Vetenskapsrådet 2018-00238.

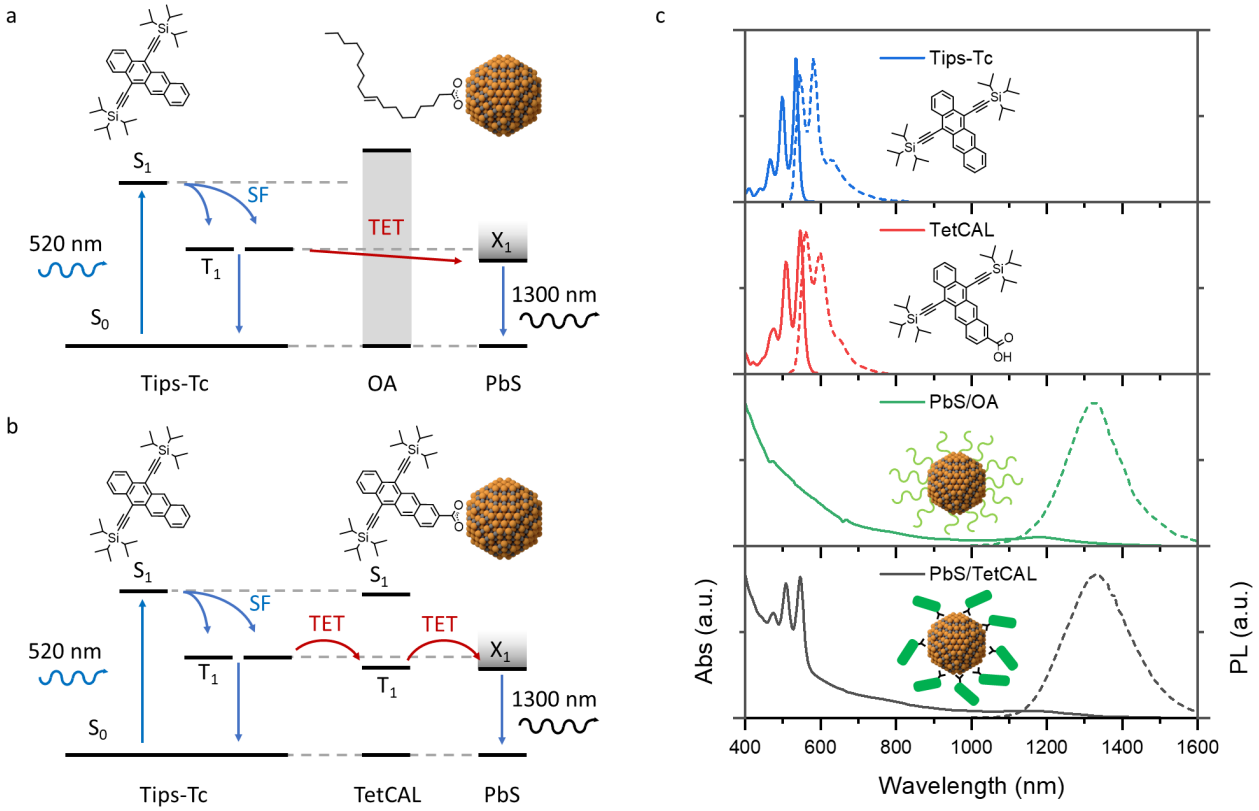

Figure 1. TIPS-Tc, TetCAL and PbS NCs act as the singlet fission material, transmitter and emitter respectively in this hybrid photon multiplier system. (a, b) Schematics of the photon multiplication process. The TIPS-Tc molecules absorb high-energy visible photons, producing a photoexcited S_1 state which then interacts with a different ground-state molecule to undergo singlet fission to form two excited triplet molecules via an intermediate TT state. (a) The high-bandgap carboxylic acid inhibits the TIPS-Tc triplets from getting close enough to the PbS NCs for triplet energy transfer (TET) to occur. (b) The TetCAL molecules bound to the PbS NCs surface are populated via TET from the TIPS-Tc, bringing the triplets in close contact with the PbS NCs and thus mediating TET to the PbS NCs. (c) The absorbance (solid line) and emission (dashed line) spectra of Tips-Tc (blue/top), TetCAL (red/top-mid), PbS-OA NCs (green/bottom-mid) and PbS-TetCAL NCs (black/bottom).

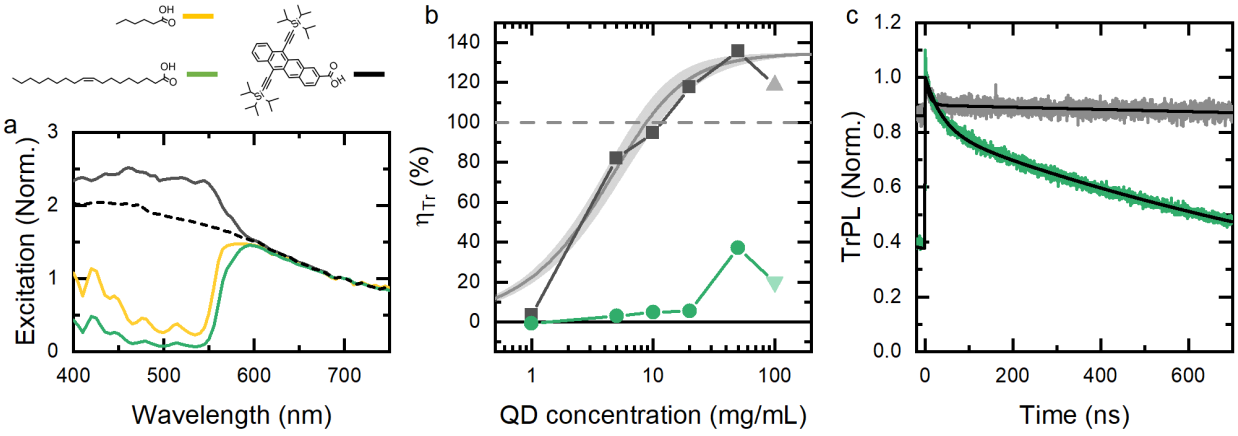

Figure 2. (a) PbS QD PL excitation spectra for solutions of TIPS-Tc (200 mg/mL) and 1.05 eV PbS QDs (50 mg/mL) with OA (green), HA (yellow) TetCAL (grey) ligands, along with PbS/OA QDs on their own (dashed). The excitation spectra are normalised to the value at 700 nm, where only the QD is absorbing. (b) Excitation transfer efficiencies from TIPS-Tc to PbS/OA (green circles) and PbS/TetCAL (black squares) in solution with varying concentrations together with TIPS-Tc (200 mg/mL), under 515 nm 500 μW/cm^2 excitation. The horizontal grey dashed line indicates the point at which 100% excitation transfer occurs. The values for 100 mg/mL QD concentration have been highlighted as outliers due to self-absorption losses. The triplet exciton transfer efficiency, ϕ_{TET}, calculated with the kinetic parameters derived from the nsTA (details below) is scaled by a singlet fission efficiency, $\eta_{SF} = 1.35 \pm 0.05$, to match with the values obtained by PLQE measurements for PbS/TetCAL (grey, with 95% confidence bounds). (c) Near-infrared transient PL for 10mg/mL PbS/OA NCs (green) and PbS/TetCAL NCs (grey) in toluene with 100 mg/mL TIPS-Tc, under excitation with 530 nm 300 pJ/cm^2, 1 MHz repetetion rate pump pulses. The kinetics have been normalised to the maximum value after removal of a fixed value representative of contributions to camera counts from ambient conditions. The laser pump timing has been aligned with $t = 0\ ns$, and thus counts before this time are residual counts from all previous pump pulses. The fits to the transient kinetics (black) follow a parameterisation with a bi-exponential function, where the slower exponential decay is summed over all previous pump pulses, representing an exponential decay in a periodic driven system (see supplementary section 7 for details).

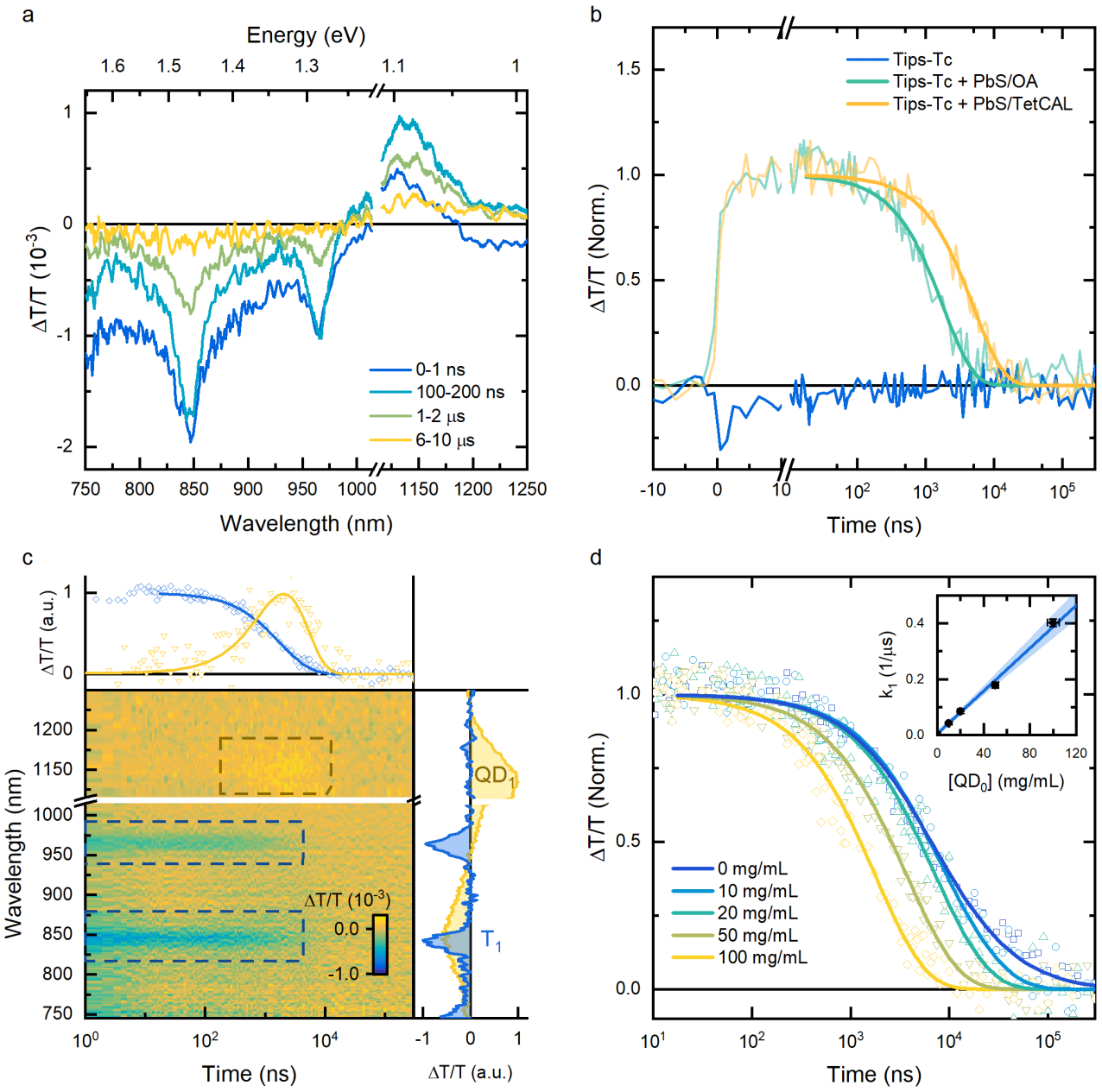

Figure 3. (a) nsTA spectra of TIPS-Tc + PbS/TetCAL blend (200 mg/mL and 100 mg/mL), excited at 532 nm 170 μJ/cm^2. Each spectrum is an average over the time ranges indicated. (b) Normalised nsTA kinetics under 40 μJ/cm^2, at the QD GSB region (1140-1160 nm). The QD GSB signals have been fitted with a mono-exponential decay. The PbS/OA and PbS/TetCAL QDs are found to decay with a 1.8 ± 0.1 and 5.1 ± 0.2 μs decay constant respectively. The 1140-1160 nm kinetic for TIPS-Tc has been scaled by the same normalised factor as for PbS/TetCAL+TIPS-Tc. (c) nsTA difference map for a solution of TIPS-Tc (200mg/mL) and PbS/TetCAL QDs (100 mg/mL), under 535 nm 40 μJ/cm^2 excitation. The PbS/TetCAL and TIPS-Tc triplet TA spectra used for decomposition by linear regression are shown (right inset). The strengths of TIPS-Tc triplet PIA signal (from linear regression) and the PbS/TetCAL QD GSB (1140-1160 nm) are shown with overlaid simulation of the population (top inset). (d) Normalised kinetics for the TIPS-Tc triplet population found from decomposition via linear regression of the corresponding nsTA difference map, for a variety of PbS/TetCAL QD concentrations. The triplet

decay kinetics are fitted with an analytical solution for a second-order rate equation, where the bimolecular triplet decay rate is a the value found for pristine TIPS-Tc. The inset shows the fitted monomolecular triplet decay rate constant as a function of PbS/TetCAL QD concentration with a linear fit and 95% confidence bounds.

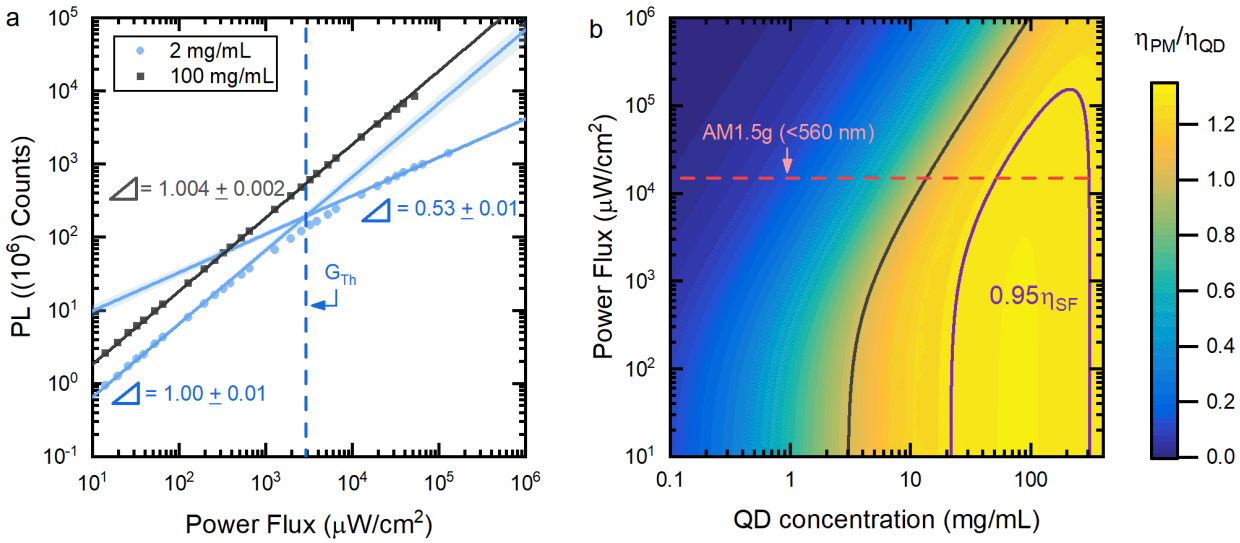

Figure 4. (a) Total IR PL counts from PbS/TetCAL QDs for solutions of low (2 mg/mL, blue circles) and high (100 mg/mL, black squares) QD concentration with TIPS-Tc (200 mg/mL) for varying 532 nm excitation flux. The PL counts are fit with power-law relations to laser flux, either across the entire flux range (100 mg/mL) or separated into two fits (2 mg/mL), for low and high photon flux. The intercept of the fits to the low and high flux regimes gives 2.9 ± 1.0 mW/cm^2 as the threshold power flux (blue vertical dashed line). (b) Simulation of the photon multiplication efficiency normalised by the PbS/TetCAL QD intrinsic PLQE, under 532 nm excitation. Two contours of interest are highlighted; the region in which the PM efficiency is larger than the QD PL efficiency η_{QD} (black) and when PM efficiency is 95% of the upper limit for PM efficiency given by the singlet fission yield (purple line). The equivalent solar flux available for absorption by TIPS-Tc under the AM1.5G spectrum (red horizontal dashed line).

References

1. Nelson, J. *The physics of solar cells*. (World Scientific Publishing Company, 2003).
2. NREL. Best Research-Cell Efficiencies. Available at: https://www.nrel.gov/pv/assets/pdfs/best-research-cell-efficiencies-190416.pdf. (Accessed: 15th May 2019)
3. Green, M. A., Emery, K., Hishikawa, Y., Warta, W. & Dunlop, E. D. Solar cell efficiency tables (Version 45). *Prog. Photovoltaics Res. Appl.* **23**, 1–9 (2015).
4. Shockley, W. & Queisser, H. J. Detailed balance limit of efficiency of p-n junction solar cells. *J. Appl. Phys.* **32**, 510–519 (1961).
5. Smith, M. B. & Michl, J. Recent advances in singlet fission. *Annu. Rev. Phys. Chem.* **64**, 361–86 (2013).
6. Xia, J. *et al.* Singlet Fission: Progress and Prospects in Solar Cells. *Adv. Mater.* **29**, (2017).
7. Merrifield, R. E. (Triplet Annihilation, Simple) Theory of Magnetic Field Effects on the Mutual Annihilation of Triplet Excitons. *J. Chem. Phys.* **48**, 4318 (1968).
8. Merrifield, R. E., Avakian, P. & Groff, R. P. Fission of singlet excitons into pairs of triplet excitons in tetracene crystals. *Chem. Phys. Lett.* **3**, 386–388 (1969).
9. Geacintov, N., Pope, M. & Vogel, F. Effect of Magnetic Field on the Fluorescence of Tetracene Crystals: Exciton Fission. *Phys. Rev. Lett.* **22**, 593–596 (1969).
10. Pope, M., Geacintov, N. E. & Vogel, F. Singlet Exciton Fission and Triplet-Triplet Exciton Fusion in Crystalline Tetracene. *Mol. Cryst. Liq. Cryst.* **6**, 83- (1969).
11. Dexter, D. L. Two ideas on energy transfer phenomena: Ion-pair effects involving the OH stretching mode, and sensitization of photovoltaic cells. *J. Lumin.* **18**–**19**, 779–784 (1979).
12. MacQueen, R. W. *et al.* Crystalline silicon solar cells with tetracene interlayers: the path to silicon-singlet fission heterojunction devices. *Mater. Horizons* **5**, 1065–1075 (2018).
13. Ehrler, B., Wilson, M. W. B., Rao, A., Friend, R. H. & Greenham, N. C. Singlet exciton fission-sensitized infrared quantum dot solar cells. *Nano Lett.* **12**, 1053–1057 (2012).
14. Congreve, D. N. *et al.* External quantum efficiency above 100% in a singlet-exciton-fission-based organic photovoltaic cell. *Science* **340**, 334–7 (2013).
15. Pazos-Outo, L. M. *et al.* A Silicon−Singlet Fission Tandem Solar Cell Exceeding 100% External Quantum Efficiency with High Spectral Stability. **08**, 7 (2019).
16. Rao, A. & Friend, R. H. Harnessing singlet exciton fission to break the Shockley–Queisser limit. *Nat. Rev. Mater.* **2**, 1–12 (2017).
17. Futscher, M. H., Rao, A. & Ehrler, B. The Potential of Singlet Fission Photon Multipliers as an Alternative to Silicon-Based Tandem Solar Cells. *ACS Energy Lett* **22**, (2018).
18. Thompson, N. J. *et al.* Energy harvesting of non-emissive triplet excitons in tetracene by emissive PbS nanocrystals. *Nat. Mater.* **13**, 1039–1043 (2014).
19. Tabachnyk, M. *et al.* Resonant energy transfer of triplet excitons from pentacene to PbSe nanocrystals. *Nat. Mater.* **13**, 1033–1038 (2014).
20. Huang, Z. *et al.* Hybrid Molecule − Nanocrystal Photon Upconversion Across the Visible and Near-Infrared. *Nano Lett.* **15**, 5552–5557 (2015).
21. Zhang, B., Liu, Y., State, B. G. & Green, B. Direct observation of triplet energy transfer from

semiconductor nanocrystals. *Science (80-.).* **351**, 369–372 (2016).

22. Mahboub, M., Maghsoudiganjeh, H., Pham, A. M., Huang, Z. & Tang, M. L. Triplet Energy Transfer from PbS(Se) Nanocrystals to Rubrene: the Relationship between the Upconversion Quantum Yield and Size. *Adv. Funct. Mater.* **26**, 6091–6097 (2016).

23. Huang, Z. & Tang, M. L. Designing Transmitter Ligands That Mediate Energy Transfer between Semiconductor Nanocrystals and Molecules. *J. Am. Chem. Soc.* **139**, 9412–9418 (2017).

24. Nishimura, N. *et al.* Photon upconversion utilizing energy beyond the band gap of crystalline silicon with a hybrid TES-ADT/PbS quantum dots system. *Chem. Sci.* **10**, 4717–4932 (2019).

25. Nienhaus, L. *et al.* Speed Limit for Triplet-Exciton Transfer in Solid-State PbS Nanocrystal-Sensitized Photon Upconversion. *ACS Nano* **11**, 7848–7857 (2017).

26. Li, X., Huang, Z., Zavala, R. & Tang, M. L. Distance-Dependent Triplet Energy Transfer between CdSe Nanocrystals and Surface Bound Anthracene. *J. Phys. Chem. Lett* **7**, 28 (2016).

27. Stern, H. L. *et al.* Identification of a triplet pair intermediate in singlet exciton fission in solution. *Proc. Natl. Acad. Sci.* **112**, 7656–7661 (2015).

28. Davis, N. J. L. K. *et al.* Singlet Fission and Triplet Transfer to PbS Quantum Dots in TIPS-Tetracene Carboxylic Acid Ligands. *J. Phys. Chem. Lett.* **9**, 1454–1460 (2018).

29. Dover, C. B. *et al.* Endothermic singlet fission is hindered by excimer formation. *Nat. Chem.* **10**, 305–310 (2018).

30. Cheng, Y. Y. *et al.* Kinetic Analysis of Photochemical Upconversion by Triplet-Triplet Annihilation: Beyond Any Spin Statistical Limit. *J. Phys. Chem. Lett* **1**, 1795–1799 (2010).

31. Huang, Z. *et al.* PbS/CdS Core-Shell Quantum Dots Suppress Charge Transfer and Enhance Triplet Transfer. *Angew. Chemie Int. Ed.* **56**, 16583–16587 (2017).

32. Shoup, D., Lipari, G. & Szabo, A. Diffusion-controlled bimolecular reaction rates. The effect of rotational diffusion and orientation constraints. *Biophys. J.* **36**, 697–714 (1981).

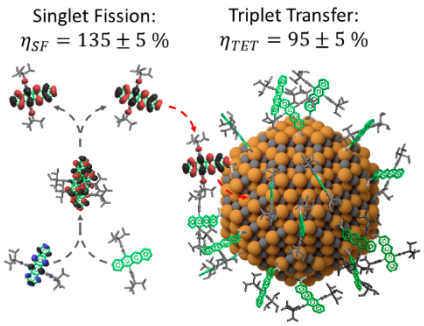

For Table of Contents Only

Supporting Information

Engineering Molecular Ligand Shells on Quantum Dots for Quantitative Harvesting of Triplet Excitons Generated by Singlet Fission

Jesse R. Allardice[a], Arya Thampi[a], Simon Dowland[a], James Xiao[a], Victor Gray[a,d], Zhilong Zhang[a], Peter Budden[a], Anthony J. Petty II[b], Nathaniel J. L. K. Davis[c,a], Neil C. Greenham[a], John E. Anthony[b] and Akshay Rao[a]

Contacts

[a]Cavendish Laboratory, University of Cambridge, J. J. Thomson Avenue, Cambridge, CB3 0HE, UK

[b]Department of Chemistry, University of Kentucky ,161 Jacobs Science Building, Lexington KY 40506-0174, USA

[c]The MacDiarmid Institute for Advanced Materials and Nanotechnology, The Dodd-Walls Centre for Photonic and Quantum Technologies, School of Chemical and Physical Sciences, Victoria University of Wellington, Wellington 6140, New Zealand.

[d]Department of Chemistry, Ångström Laboratory, Uppsala University, Box 532, SE-751 20 Uppsala, Sweden

1 Contents

2 Methods

2.1 Chemicals

The TIPS-Tetracene-Carboxylic acid (TetCAL) was synthesized as described previously.[1] The TIPS-Tc was obtained from Ark Pharm. All other chemicals were purchased from Sigma-Aldrich and used as delivered.

The synthesis of PbS QDs was carried out following a modified version of previously reported methods.[2] Briefly, PbO (0.45 g), oleic acid (7 g) and 1-octadecene (10 g) were loaded in a three-neck flask and degassed at 110 °C for 2 h. Subsequently, the reaction flask was flushed with nitrogen and the temperature was lowered to 95 °C. A solution containing bis(trimethylsilyl)sulphide (210 µL) in 1-octadecene (5 mL) was rapidly injected into the lead precursor solution. The reaction flask was then allowed to cool down naturally to ambient temperature (~25 °C). The PbS QDs were first extracted by adding hexane and acetone, followed by centrifugation. Before ligand exchange, the QDs were further purified with hexane/acetone and then re-dispersed in toluene at a concentration of ~100 mg mL^{-1}.

The ligand exchange was performed in a nitrogen-filled glovebox. The PbS QDs stock solution was diluted to ~20 mg mL^{-1} and 1 mL was used for ligand exchange. 0.2 mL of the TetCAL solution (variable amounts dissolved in tetrahydrofuran) was added to the PbS QD solution, and the mixture was stirred for at least 1 h. The PbS/TetCAL QDs were then extracted by adding acetone (4.8 mL) to the mixture followed by centrifugation. The supernatant was discarded and the precipitated QDs were re-dispersed in toluene (1 mL). The PbS/TetCAL QDs were further purified using a minimum of six repeated dispersion/precipitation/centrifugation cycles until the wash solution contained no TetCAL. Finally, PbS/OA or PbS/TetCAL QDs at varying concentration (up to 100 mg mL^{-1}) and TIPS-Tc (200 mg mL^{-1}) were dispersed in toluene and dispensed into cuvettes under a nitrogen atmosphere.

2.2 Optical Spectroscopy

2.2.1 Continuous Wave Measurements

Absorbance spectra of solutions were measured using a Shimadzu UV3600Plus spectrometer with attached integrating sphere. Photoluminescence excitation spectra were measured on an Edinburgh Instruments FLS980 fluorimeter. Solution samples were measured using in-house made cuvettes with optical path length on the order of 100 microns thick.

2.2.2 PL Quantum Efficiency Measurements

PLQE measurements were made following the procedure of de Mello et al.[3] Temperature and current controlled laser diodes (Thorlabs) were used to generate stable laser beams with wavelengths either 515 nm or 658 nm. After attenuation to the desired intensity these were aligned through a small hole, onto samples suspended, in a Spectralon-coated integrating sphere (Newport 819C-SL-5.3) modified with a custom baffle extension. Light from the experiment was collected using an optical fibre connected to a Andor Kymera 328i Spectrograph and spectra recorded using either a Si-CCD (Andor iDus 420) for the visible region, or a InGaAs detector (Andor, Dus InGaAs 490) for the NIR region.

2.2.3 Steady State IR PL and Magnetic Dependent PL

Temperature and current controlled laser diodes (Thorlabs) were used to generate stable 530 nm and 658 nm laser beams. After attenuation to the desired intensity the laser beam was focused onto the sample cuvettes while PL light from the sample was collected and focused into a Andor Kymera 328i Spectrometer and spectra recorded using either a Si-CCD (Andor iDus 420) for the visible region, or a InGaAs detector (Andor, Dus InGaAs 490) for the NIR region. Additionally when magnetic field dependent PL measurements were performed an

electromagnet was place such that the sample was located within the poles of the electromagnet. As described previously, different magnetic field strengths were achieved by using a Keithley 2400 variable voltage source connected to a current amplifier, to drive the electromagnet.[4] The magnetic field between the poles (at the sample position) was calibrated to the applied voltage by a Gauss-meter. When measuring the PL, from the PbS QDs (near IR region), both a RG1000 long pass filter (Schott) and a PL950 long pass filter (Thorlabs) were placed in front of the entrance to the spectrometer. These removed laser scatter and higher order peaks from the grating. After averaging over multiple sweeps of the magnetic field and integration of the spectra, the percentage change relative to the spectrum under zero applied field strength was calculated.

2.2.4 Transient Absorption

In this technique a pump pulse generates photoexcitations within the solutions, which are then probed at later times using a broadband probe pulse. Transient absorption spectra were recorded over short (200 fs - 2 ns) and long (1 ns- 300 μs) time delays. The femtosecond transient absorption experiments are performed using an Yb- based amplifying system, Light Conversion PHAROS with 400 μJ per pulse at 1030 nm with a repetition rate of 38 kHz. The laser output is modified using a 4 mm YAG substrate to produce the probe beam from 520 to 950 nm. Using a narrow band optical parametric oscillator system (ORPHEUS- LYRA, Light conversion) with 1030 nm seed, the pump beam is generated at 535 nm (full-width at half-maximum 250 fs). The probe pulse is delayed using a computer- controlled mechanical delay-stage (Newport) and the on-off pump pulses are generated by means of a mechanical chopper (Thorlabs) before hitting the sample. The pump and probe beams are focused with sizes 250x250 μm and 80x80 μm respectively, at the sample position. The probe pulse transmitted through the sample cuvette is collected using a silicon line scan camera (AViiVA EM2/EM4) with a visible monochromator 550 nm blazed grating.

For long-time (ns-TA) measurements a LEUKOS Disco 1 UV Low timing jitter supercontinuum laser (STM-1-UV) is used to generate the probe. This laser produces pulses with a temporal breadth below 1 ns from 200-2400 nm and has an electronically controlled delay relative to the pump. The pump is generated at the desired wavelength using a TOPAS optical amplifier pumped by 800 nm 100 fs pulses from the Spectra-Physics Solstice Ace Ti:Sapphire amplifier at 1 kHz. The probe is split by a 50% reflectance beam splitter to create a reference. The pump and probe beams are overlapped on the sample adjacent to the reference beam. This reference is used to account for any shot-to-shot variation in transmission. The sample is held in a 1 mm quartz cuvette, mounted into a holder. The probe and reference beams are focused into an imaging spectrograph (Andor, Shamrock SR 303i) and detected using a pair of linear image sensors (Hamamatsu, G11608) driven and read out at the full laser repetition rate by a custom-built board from Stresing Entwicklungsburo. In all measurements every second pump shot is omitted using a mechanical chopper for short-time measurements. The average fractional differential transmission (ΔT/T) of the probe is calculated for each time delay once 1000 shots have been collected. Deconvolution of TA data is achieved using either spectral target analysis or global analysis. For spectral target analysis we predefine the spectra present and find the proportion of each spectrum present at every time point via linear regression. While, global analysis of the TA data is achieved using a genetic algorithm described previously.[5,6]

2.2.5 IR TCSPC

Samples were excited with a pulsed supercontinuum laser (Fianum Whitelase SC-400-4, 6 ps pulse length) at 1 MHz repetition rate. The pump wavelength set to 530 nm (full-width at half-maximum 10 nm) with a dielectric filter (Thorlabs). Pump scatter from the laser excitation within the photoluminescence path to the detector was filtered-out with an absorptive 1000 nm long-pass filter (Thorlabs). The infrared photoluminescence was focused and detected by a single-photon avalanche photodiode based on InGaAs/InP (MPD-InGaAs-SPAD).

2.3 Solution Preparation

Cuvettes of three varying thickness' were used during optical measurements. Experiments requiring a fixed and accurate path length, 1 mm cuvettes (Sigma-Aldrich Hellma absorption cuvette) were used. The disadvantage of these cuvettes is that their long optical path length means concentrated solution are incredibly optically dense in the visible region and thus effectively no visible light can be transmitted. Even in situations where transmission is not important, the amount of material required for use is excessive.

To reduce the path length in-house made cuvettes were used. Cuvettes with roughly 100 µm gaps were created by stacking a 100 µm thick PVC sheet, stencilled with a cavity, between to glass cover slides. The edges were encapsulated with a 2-part quick dry epoxy (Araldite 2-part epoxy adhesive). The advantage of this particular sized cuvette is that the solution inside is of high enough optical density for reliable QD PLQE values to be achieved with excitation across the visible range.

However, to achieve a SF-PM with low parasitic QD absorption (560-1200 nm) cuvettes with no spacer were used during the absorption measurements. These samples have a gap for solutions on the order of 10 µm, as determined form comparison of absorbance values with a TIPS-Tc reference solution.

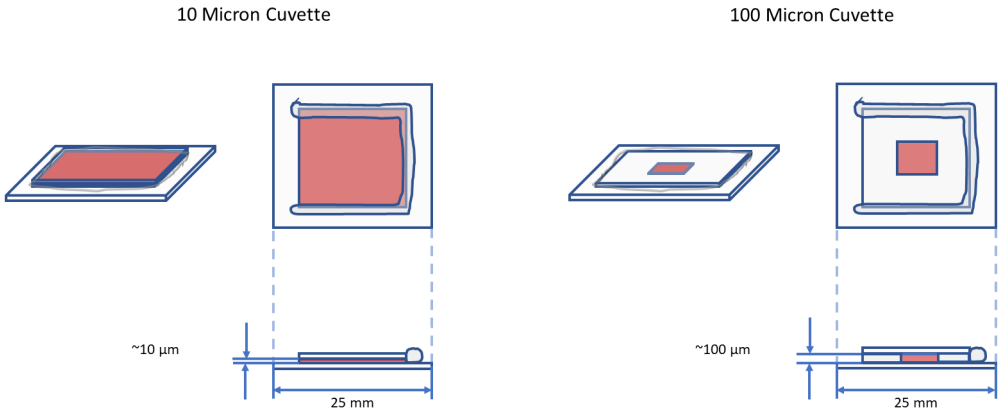

Figure S1: Schematic of the in-house made cuvettes, both were filled with roughly 10 µL of solution. The low volumes needed for these cuvettes allows the exploration of a wider range of concentration, particularly for higher concentrations of TIPS-Tc and QDs where material constraints must be considered. After filling the cavity with the desired solution, epoxy was applied to seal the remaining edge.

3 Absorption Measurements

3.1 PbS Molar Mass Estimation

Estimation of the number of ligands attached to the surface of a quantum dot is experimentally challenging and can be achieved with techniques such as DOSY NMR.[7] Here, when estimating the molar mass of PbS-OA, we include the mass of 130 oleic acid ligands attached to the surface of each QD.[8] From TEM done in previous work we used a QD diameter of 3.4 ± 0.3 nm.[9] By modelling the QD as a sphere and combining it with the bulk density of PbS of 7.6 g/cm^3,[10] and 130 oleic acid ligands per QD, we calculate a molar mass of 130000 ± 20000 g/mol. We use this value to convert between grams and moles of PbS quantum dots. There are more sophisticated methods in the literature that take into account non-stochiometric ratios of Pb and S, however we leave these methods to future work.[11]

3.2 QD Molar and Mass Attenuation Coefficient

Using a 1mm cuvette with dilute solutions of TIPS-Tc, PbS-OA and PbS-TetCAL at 2 mg/mL in toluene the absorbance spectra were measured on a Shimdzu UV-3600-Plus with integrating sphere (ISR-603 integrating

sphere attachment). Starting from the known mass concentrations, the absorbance spectra and molar masses, we estimate the molar attenuation coefficient via the Beer-Lambert law in the form,

$$\epsilon = \frac{A \cdot M}{l \cdot \rho}.$$

Where ϵ is the molar attenuation coefficient, A is the absorbance, l is the path length, M is the molar mass and ρ is the mass concentration. The obtained molar and mass absorption spectra are shown in figure S2 a and b. At 400 nm we estimate molar absorption coefficient of roughly $\epsilon \sim 5 \times 10^6$ (L mol^{-1} cm^{-1}) for both OA and TetCAL QDs, which is slightly lower than previously stated values of $\epsilon \sim 10 \times 10^6$ (L mol^{-1} cm^{-1}) for similar QDs.[11]

Using the molar attenuation coefficients of TIPS-Tc and the QDs we calculate the fraction of absorbed photons for each component as a function of wavelength. Figure S2.b shows the fraction of photons absorbed by the TIPS-Tc molecules in a solution of TIPS-Tc (200 mg/mL) and PbS/TetCAL (100 mg/mL).

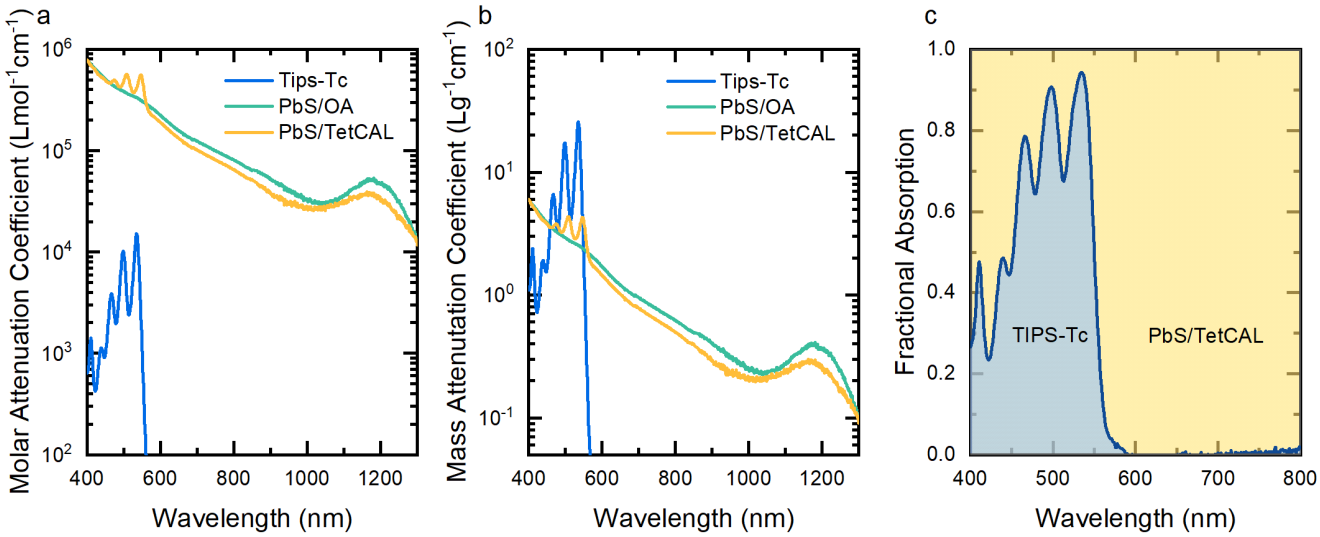

Figure S 2: Molar (a) and mass (b) attenuation coefficients of TIPS-Tc, PbS-OA QDs and PbS-TetCAL QDs. (c) Predicted TIPS-Tc fractional absorption in a solution of TIPS-Tc (200 mg/mL) and Pbs/TetCAL (100 mg/mL).

3.3 Laser Penetration Depth

Using the molar attenuation coefficient calculated from the absorbance measurement, we calculate, δ_P, the penetration depth by,

$$\delta_P = \frac{M}{\epsilon \rho \ln(10)}.$$

For TIPS-Tc (200 mg/mL) under 535 nm excitation, $\epsilon = 15200\ L\ mol^{-1} cm^{-1}$, and at 200 mg/mL we calculate a penetration depth of 0.86 µm. Adding PbS QDs at the concentrations used in this work, it is calculated to have small effect on δ_P, reducing the penetration depth by less than 6% (Figure S3).

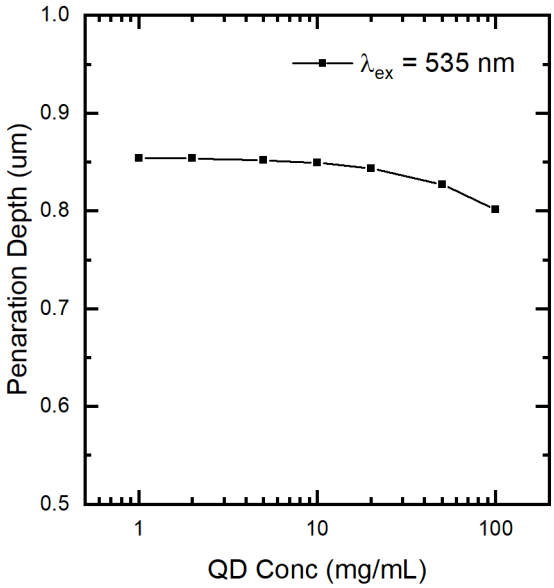

Figure S 3. Calculated light penetration depth (535nm) for solutions of PbS/TetCAL QDs and TIPS-Tc (200 mg/mL). The values are calculated from the measured attenuation coefficients.

3.4 Calculation of the QD Parasitic Absorption

Absorption of light directly to QDs is considered parasitic, as the exciton multiplication step is absent, resulting in sub-optimal performance of the underlying PV. This parasitic absorption has the largest effect at wavelengths below the bandgap of the singlet fission material, where the QDs have non-negligible absorption and are the exclusive absorbing material in the SF-PM.

An upper limit for this parasitic absorption in a "realistic" SF-PM implementation has been up at 5%. With the condition that the SF-PM still be optically dense enough for the singlet fission material's absorption to be 95%.[12] Figure S4.a shows the absorbance spectrum for a solution of TIPS-Tc (200 mg/mL) and PbS/TetCAL QDs (50 mg/mL) in a in house made micro cuvette. Fitting with the measured attenuation spectra (Figure S2) to this reveals that the path length of the cuvette is 15 ± 2 µm. This illustrates that we can achieve path lengths on the micron scale and that absorbance in our SF-PM is orders of magnitude higher in the singlet fission material (535 nm) than in the parasitic QD absorption range (>560 nm). There exist methods for producing solutions as thin as 2 µm, we leave it to future work to demonstrate such thickness' with a solution SF-PM.[13,14] However, via calculation we find that a 2.5 µm thick solution would absorb 95% of the light at the TIPS-Tc absorption peak and keep the QD parasitic absorption (>560 nm) less than 5% (figure S4.c and d).

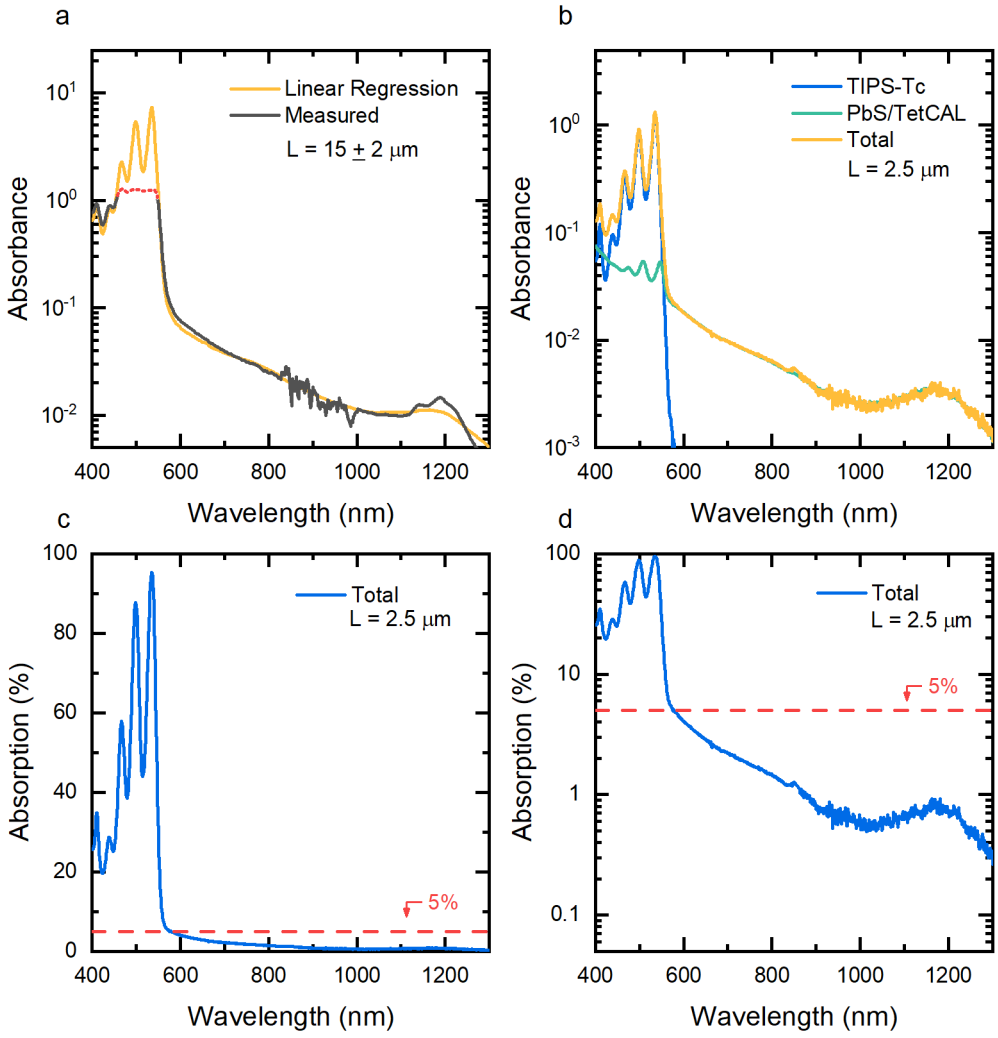

Figure S 4. a) Measured absorbance of a SF-PM solution (black) with 200 mg/mL of TIPS-Tc and 50 mg/mL of PbS/TetCAL QDs. Due to the extremely high absorption at the TIPS-Tc absorption peak and the limited sensitivity of the measurement, the true value for the TIPS-Tc absorbance peak is not captured (red dashed). The measured attenuation spectra of TIPS-Tc and PbS/TetCAL, combined at the appropriate concentration and have been fitted (by linear regression) to the valid region of the measured absorbance spectrum. From the known attenuation coefficient of TIPS-Tc we calculate the thickness of this "micro cuvette" as 15 ± 2 µm. b) Using the attenuation

spectra for TIPS-Tc and PbS/TetCAL we calculate the attenuation spectrum for a 2.5 μm thick, TIPS-Tc (200 mg/mL) and PbS/TetCAL (50 mg/mL), singlet fission photon multiplier solution. From this we calculate the percentage absorption for this PM solution (c,d), and show that the QD parasitic absorption, in the region below the singlet fission material absorption band ($\lambda > 560$ nm), is less than 5 % (horizontal: dashed red). While the TIPS-Tc Absorption (535 nm) is as high as 95%.

4 PLQE

Excitation wavelength	515 nm						658 nm
QD Conc (mg/mL)	1	5	10	20	50	100	20
PbS/OA	0.0	1.1	2.0	3.1	10.1	9.9	19.2
PbS/TetCAL	0.6	12.0	13.8	16.7	18.2	16.0	14.6

Tabel S 1. IR PLQE values for solutions of TIPS-Tc (200 mg/mL) and QD's of varying concentration, under 515 and 658 nm laser excitation. The intrinsic QDs PLQE is taken as the IR PLQE under 658 nm excitation, in a solution of TIPS-Tc (200 mg/mL) and QDs (20 mg/mL). 515 and 658 nm IR PLQE values were measured under 500 µW/cm² fluence.

The expected IR PLQE of the SF-PM solutions without exciton transfer is given by,[15]

$$\eta_{k_{Tr=0}}(\lambda) = \eta_{QD}\frac{\mu_{QD}(\lambda)}{\mu_{QD}(\lambda)+\mu_{Tc}(\lambda)}.$$

Where η_{QD} is the intrinsic PLQE of the QDs (658 nm excitation), μ_i is the attenuation coefficient base 10, of the ith component. The measured molar attenuation coefficients and the intrinsic QDs PLQE are used to calculate this "no transfer case" for the IR PLQE (Figure S5). This illustrates the minimum amount of IR PL that will be observed in the solutions, values higher than this indicate exciton transfer.

Alternatively the exciton transfer efficiency, η_{Tr}, can be calculated from,[15]

$$\eta_{Tr}(\lambda) = \frac{1}{\mu_{Tc}(\lambda)}\left(\frac{\eta_{PM}(\lambda)}{\eta_{QD}}\Big(\mu_{QD}(\lambda)+\mu_{Tc}(\lambda)\Big)-\mu_{QD}(\lambda)\right).$$

This explicitly gives the efficiency of exciton transfer from the TIPS-Tc to the QDs, in terms of the intrinsic QD IR PLQE (658 nm excitation), the SF-PM IR PLQE (excitation at λ) and the attenuation coefficients of the TIPS-Tc and QDs.

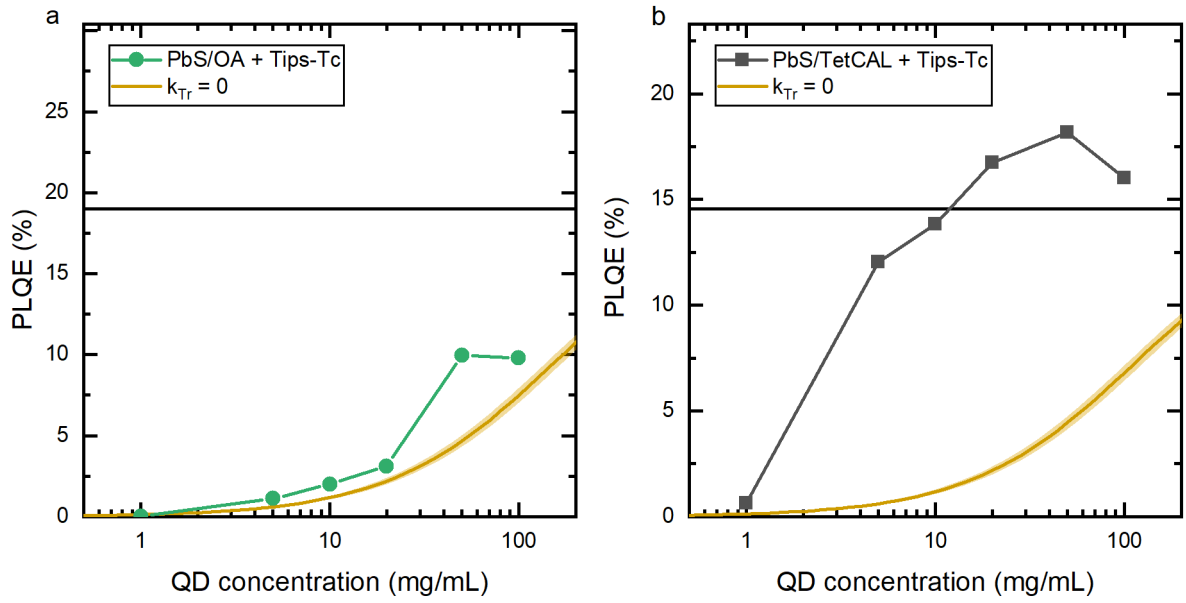

Figure S 5: IR PLQE of TIPS-Tc (200 mg/mL) with (a) PbS/OA and (b) PbS/TetCAL solutions, under 515 nm excitation. The horizontal black lines indicate the intrinsic IR PLQE of the QDs, measured under 658 nm excitation. The yellow lines indicate the expected PLQE for the solution due to photon absorption directly to the QDs (no exciton transfer). The IR PLQE with 515 nm excitation, were measured under 500 µW/cm² fluence.

The observed drop in the IR PLQE values for the SF-PM solutions at high QD concentrations is assigned to self-absorption losses. The drop in IR PLQE aligns with a red shifting of the QD's PL peak, a sign of self-absorption (Figure S6).[16]

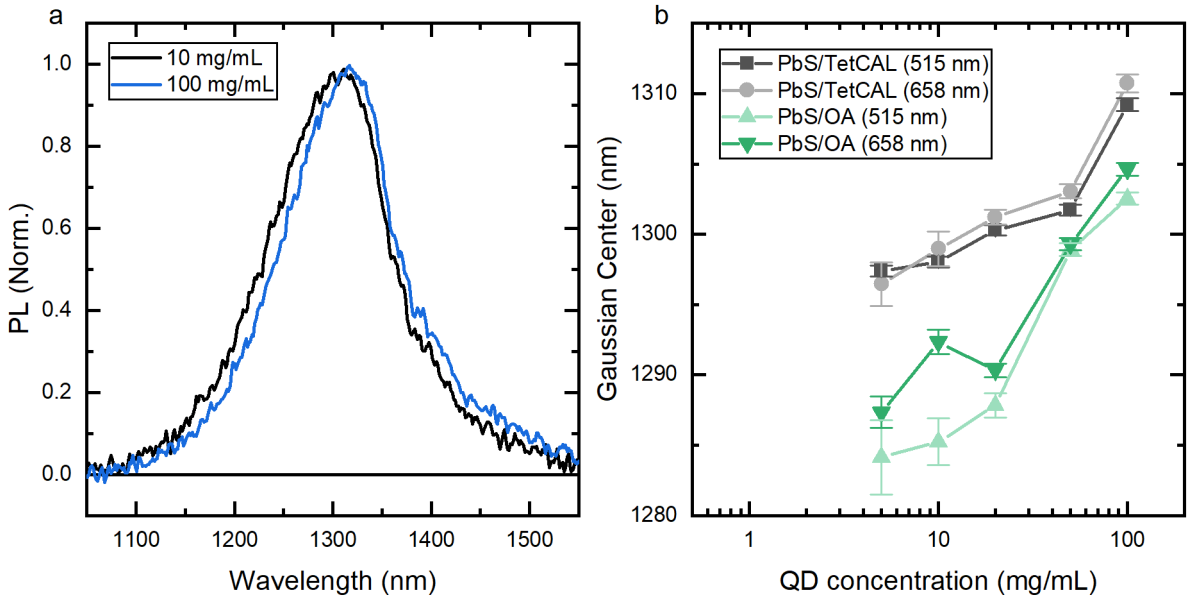

Figure S 6: a) IR PL spectra of 10 (black) and 100 mg/mL (blue) PbS/TetCAL QDs with TIPS-Tc (200 mg/mL), under 515 nm excitation, showing a red-shift in the PL for higher concentration of QDs. b) PL peak wavelength, with uncertainty, as measured by a Gaussian fit to the IR PL, for both 515 and 658 nm excitation of solution of QDs with TIPS-Tc (200 mg/mL).

5 Kinetic Modelling

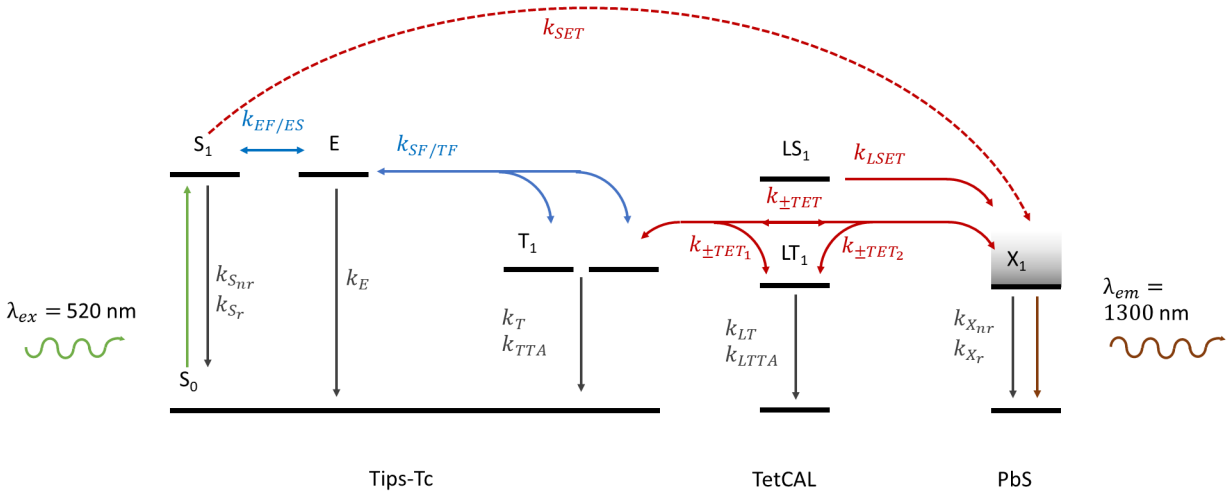

Figure S 7: Kinetic scheme illustrating some of the possible excited state process that could occur in a solution of TIPS-Tc and PbS QD with TetCAL ligand.

By taking the basic kinetic scheme for singlet fission and including a variety of interactions with a PbS/TetCAL QD we arrive at the kinetic scheme shown in figure S7.[17] These interactions include singlet exciton transfer (SET) from the TIPS-Tc (k_{SET}) and TetCAL (k_{LSET}) to the QD excitated state X_1; triplet exciton transfer (TET) in either direction between TIPS-Tc and TetCAL ($k_{\pm TET_1}$), TetCAL and the PbS QD ($k_{\pm TET_2}$) or directly between TIPS-Tc and the PbS QD ($k_{\pm TET}$). The decay channels included are TIPS-Tc singlet radiative and non-radiative decay (k_{S_r} and $k_{S_{nr}}$); PbS QD radiative and non-radiative decay (k_{X_r} and $k_{X_{nr}}$) and TIPS-Tc excimer, TIPS-Tc triplet, TetCAL triplet monomeric decay (k_E, k_T and k_{LT}). Critically we take care to include TIPS-Tc triplet bi-molecular decay via the k_{TTA} rate. Many of these processes have been shown to occur previously.[1,17] However, this is not an exhaustive list of the possible processes.[18] Analysis of the above scheme leads to the follow system of differential equations,

$$\frac{dS_1}{dt} = -\left(k_{S_{nr}} + k_{S_r} + k_{SET}\right)S_1 - k_{EF}S_0S_1 + k_{ES}E + I(\lambda)\alpha_{Tc}(\lambda)\,,$$

$$\frac{dE}{dt} = k_{EF}S_0S_1 + k_{TF}T_1^2 - (k_{E,r} + k_{E,nr} + k_{ES} + k_{SF})E\,,$$

$$\frac{dT_1}{dt} = 2k_{SF}E + k_{-TET_1}LT_1 + k_{-TET}S_0X_1 - (k_T + k_{TET_1}X_0 + k_{TET}X_0)T_1 - (k_{TTA} + 2k_{TF})T_1^2\,,$$

$$\frac{dLS_1}{dt} = -k_{LS}SL_1 - k_{LSET}SL_1 + I(\lambda)\alpha_L(\lambda)\,,$$

$$\frac{dLT_1}{dt} = k_{TET_1}T_1 + k_{-TET_2}X_1 - (k_{LT} + k_{-TET_1} + k_{TET_2})LT_1 - k_{TTLA}LT_1^2\,,$$

$$\frac{dX_1}{dt} = -\frac{dX_0}{dt} = k_{SET}S_1 + k_{TET_2}LT_1 + k_{TET}X_0T_1 + k_{LSET}SL_1 - \left(k_{X_{nr}} + k_{X_r} + k_{-TET_2} + k_{-TET}S_0\right)X_1 + I(\lambda)\alpha_{QD}(\lambda)\,.$$

Where S_0, S_1, E, T_1, LS_1, LT_1, X_0 and X_1 are respectively the density of the TIPS-Tc ground state, TIPS-Tc first excited singlet state, TIPS-Tc excimer state, TIPS-Tc triplet state, TetCAL first excited singlet state, TetCAL triplet state, PbS QD ground state and PbS QD excited state. $I(\lambda)$ is the density of photons absorbed by the sample as a function of the excitation wavelength λ and α_i is the fraction absorbed by the *ith* component.

In previous work it has been shown that the TIPS-Tc singlet decays within 100 ps in concentrated solutions.[17,18] SET from TIPS-Tc to the PbS QD can occur during this initial decay of the singlet or from singlets regenerated via triplet-triplet annihilation (TTA) in the TIPS-Tc. However, these two processes can be distinguished via their characteristic fluence dependence. SET from the initial photo excitation singlet exciton will occur at a constant efficiency determined by the branching ratio, $k_{SET}/(k_{S_{nr}} + k_{S_r} + k_{SET} + k_{EF}S_0)$, at all fluences. However, SET from TTA generated singlets will happen after 100 ps and will increase superlinear with fluence, significant populations of excited singlet excitons only being regenerated at high fluences. Later in section 8 we show that SET from the photon generated singlet is not efficient in this system (< 5%) and so the dominant process occurring at low incident fluences for the TIPS-Tc singlet is singlet fission.

We simplify the above kinetic scheme by applying the following constraints on the triplet transfer and singlet fission processes. The QD band gap is chosen such that it is lower than the TIPS-Tc and TetCAL triplet energies, making TET from the TIPS-Tc and TetCAL to the PbS QD energetically favourable over the reverse process. The singlet fission process is negligibly affected by the addition of the QDs, production of the singlet via TTA is excluded and SET from the TIPS-Tc singlet is inefficient. Exciton transfer is proceeding after singlet fission has occurred, meaning singlet fission can be treated as a unidirectional process that instantaneously produces triplets with a yield of η_{SF}. Triplet transfer from the TIPS-Tc to the TetCAL ligand is slow compared to transfer from the TetCAL ligand to the PbS QD, meaning k_{TET_2} is not the rate limiting step and so there is negligibly population of the TetCAL triplet state during the transfer step. Any photo generated excitons on the TetCAL ligand are transferred with unity efficiency to the PbS QD. This is justified by the effective equivalence of the measured IR PLQE values of the PbS/TetCAL QDs when excited at wavelengths where the TetCAL and QD absorb (515 nm) and where only the QD absorbs (658 nm), 14.2% and 14.6% respectively. In previous reports, singlet fission has been reported to occur on the surface of PbS QDs in the TetCAL ligands, we do not observed this with the QDs used in this work and assign the difference to a lower TetCAL surface coverage resulting in weaker TetCAL-TetCAL interactions.[9] Finally, we consider the the population of PbS QDs excited states as a weak perturbation of the QD ground state population and so treat X_0 as a constant.

Under these simplifications the kinetic model can be expressed as three separable efficiencies, η_{SF}, η_{TET} and η_{QD}, described by the following system of equations,

$$\frac{dT_1}{dt} = \eta_{SF} I(\lambda)\alpha_{Tc}(\lambda) - (k_T + k_{TET}X_0)T_1 - k_2 T_1^2 \,,$$

$$\frac{dX_1}{dt} = k_{TET}X_0 T_1 - \left(k_{X_{nr}} + k_{X_r}\right)X_1 + I(\lambda)\alpha_{QD+L}(\lambda) \,,$$

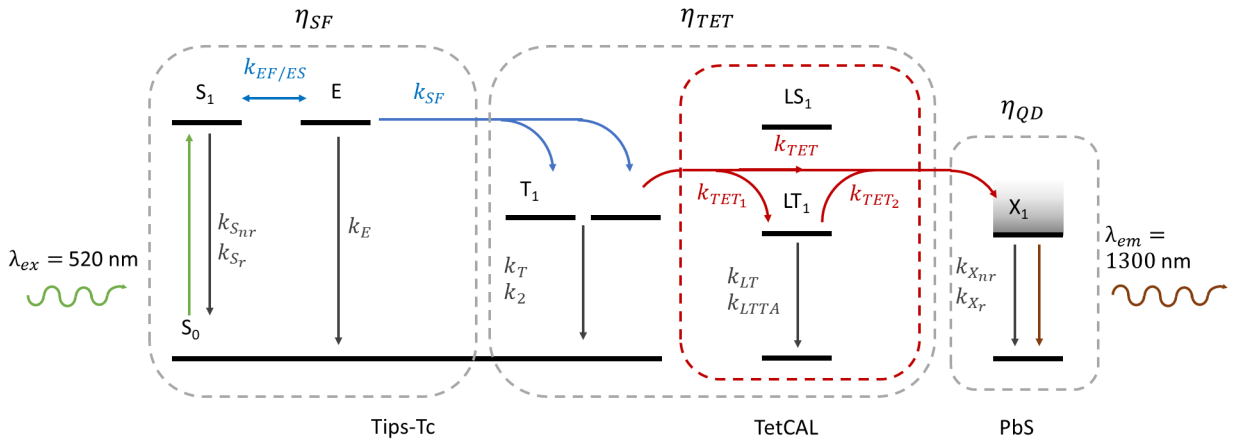

Figure S 8: Simplified kinetic scheme, where the singlet fission and triplet transfer processes are assumed to be unidirectional.

6 Diffusion Limited Reactions

The rate of reaction between spices A and B for a diffusion limited process is given by,[19]

$$k_{AB} = 4\pi(D_A + D_B)(R_A + R_B)\,.$$

Where D and R are the diffusion coefficient and radius of interaction for each component. Using this formula we show below a variety of the calculated diffusion controlled reaction rates for our solution SF-PM system. Here we take the diffusion coefficient for TIPS-Tc molecules in concentrated solution (200 mg/mL) as 5×10^{-10} $m^2 s^{-1}$ in toluene and the interaction radius as the radius of the molecule.[17] From Graham's law of diffusion we estimate that the diffusion coefficient of TIPS-Tc molecules is at least 10 times larger than for PbS QDs, based on their relative molar masses. Thus, for the purpose of estimating the rate of triplet transfer we can use the approximation of no QD diffusion.

Process	A	B	D_A (m^2/s)	D_B (m^2/s)	R_A+R_B (m)	k ($Lg^{-1}\mu s^{-1}$)	[B] (mg/mL)	k[B] (1/μs)
Singlet Fission	TIPS-Tc	TIPS-Tc	5E-10	5E-10	1.2E-09	15	200	3100
Triplet Transfer	TIPS-Tc	PbS/TetCAL	5E-10	0	2.95E-09	0.085	100	8.5

Tabel S 2: Collection of estimated bimolecular rate constants for singlet fission in TIPS-Tc and triplet exciton transfer from TIPS-Tc to PbS/TetCAL QDs in solution. For particular concentrations of interest for our solution SF-PM we calculate the reaction rate, $k[B]$. The corresponding measured singlet fission rate for TIPS-Tc was measured to be 14100 ± 800 μs^{-1}, indicating that the estimated rates are of the correct order of magnitude.

7 Transient PL Kinetic Model

We consider a process that instantaneously produces B excited states at periodic interval T, which then exponentially decay with time constant τ, the population of total excited states at time t can be expressed as,

$$y(t) = Be^{-t/\tau} + Be^{-\frac{T}{\tau}} + Be^{-\frac{2T}{\tau}} + Be^{-\frac{3T}{\tau}} + \cdots$$

Collecting the summation we find,

$$y(t) = Be^{-t/\tau}\left(1 + \sum_{n=1}^{\infty} exp\left(-\frac{nT}{\tau}\right)\right).$$

The summation is of geometric form and so the converges to,

$$\sum_{n=1}^{\infty}(e^{-x})^n = \frac{e^{-x}}{1-e^{-x}} = \frac{1}{e^x - 1},$$

for $x > 0$. Thus the population is given by,

$$y(t) = Be^{-t/\tau} + \frac{B}{e^{T/\tau} - 1}.$$

Extending this to a bi-exponential decay process with times constants τ_1 and τ_2 gives,

$$y(t) = Ae^{-t/\tau_1} + \frac{A}{e^{T/\tau_1} - 1} + Be^{-t/\tau_2} + \frac{B}{e^{T/\tau_2} - 1}.$$

In the case that τ_1 is very fast, the limit $T/\tau_1 \rightarrow \infty$, we finally arrive at,

$$y(t) \approx Ae^{-t/\tau_1} + Be^{-t/\tau_2} + \frac{B}{e^{T/\tau_2} - 1}.$$

We use this function was used to describe the QD IR transient PL. The τ_1 rate parameterise a fast decay of PL, due possibly to auger recombination, while the longer τ_2 decay represents the PL decay of the QD including population after triplet transfer. Fitting to the IR transient PL is achieved by least square fitting as shown in figure S9.b and parameters shown in table S3.

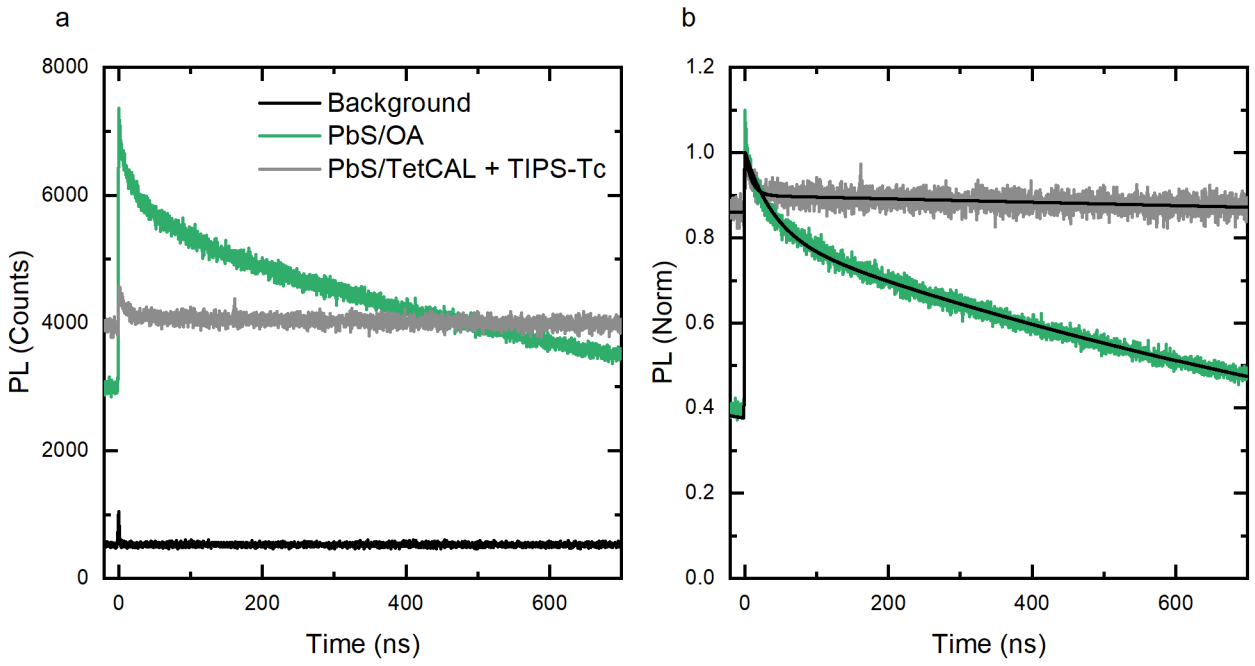

Figure S 9: a) Transient near-infrared photoluminescence counts for 10 mg/mL PbS/OA NCs (green) and PbS/TetCAL QDs (grey) in toluene with 100 mg/mL TIPS-Tc, under excitation with 530 nm 300 pJ/cm^2, 1 MHz reputition rate pump pulse. The black curve is the counts collected from ambient background, for the same collection time without any sample present in the beam path. b) The kinetics have been normalised to the maximum value after removal of a fixed value representative of contributions to camera counts from ambient conditions. The laser pump timing has been aligned with t=0 ns, and thus counts before this time are residual counts from all previous pump pulse. The fits to the transient kinetics (black) follow a parameterisation with a bi-exponential function, where the slower exponential decay is summed over all previous pump pulses, representing an exponential decay in a periodic driven system.

Sample	τ_1 **(ns)**	τ_2 **(µs)**
PbS	40 ± 1	1.300 ± 0.005
PbS/TetCAL + TIPS-Tc	10 ± 1	22 ± 0.7

Tabel S 3: Transient near-infrared photoluminescence fitting parameters for 10 mg/mL PbS/OA NCs and PbS/TetCAL QDs in toluene with 100 mg/mL TIPS-Tc, under excitation with 530 nm 300 pJ/cm^2, 1 MHz reputition rate pump pulse.

8 Transient Absorption

8.1 Femtosecond Transient Absorption

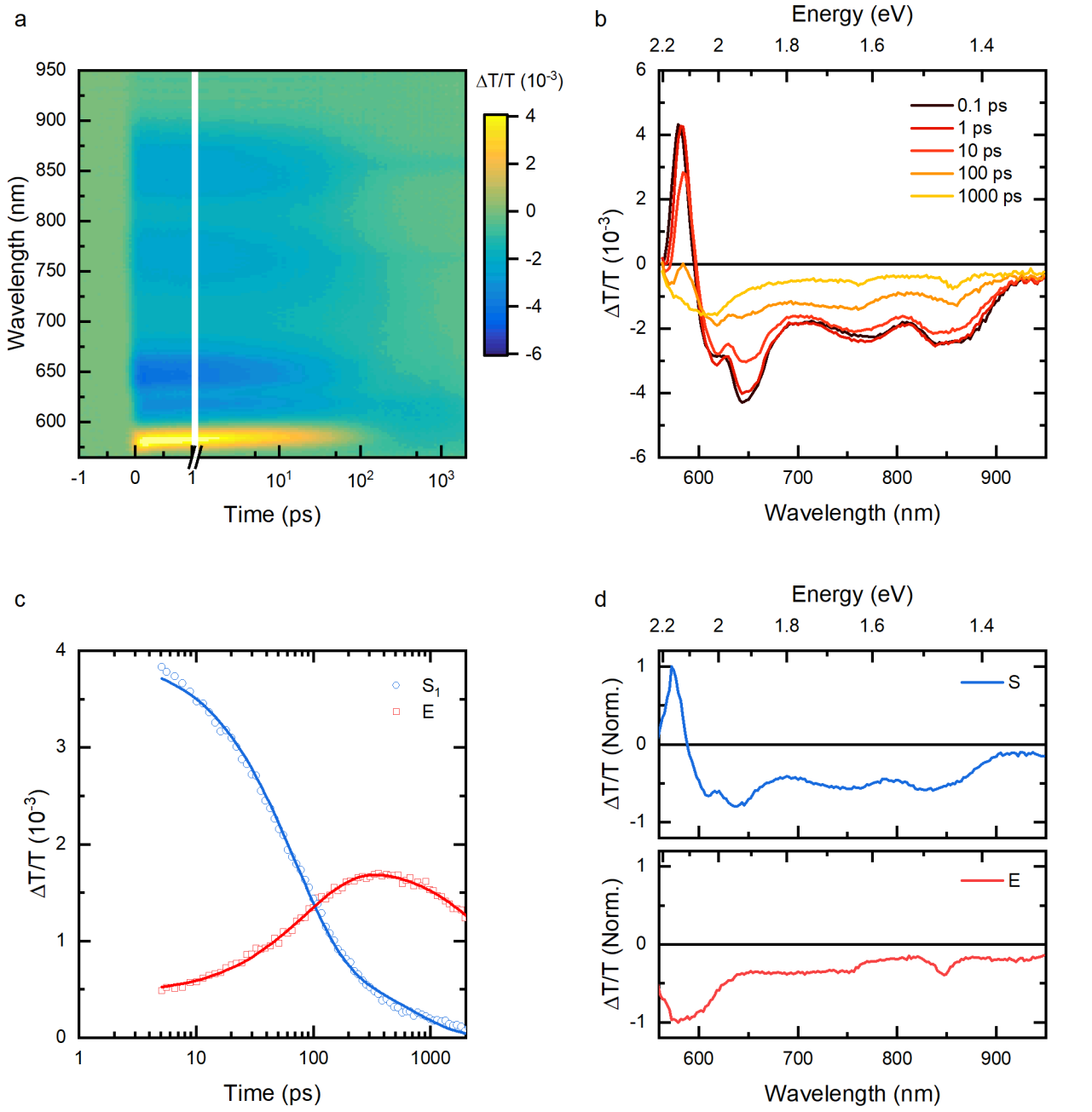

Figure S 10: Femtosecond transient absorption map (a) and spectra (b) of ~100 micron thick TIPS-Tc solution (200 mg/mL). The sample was excited with a 15 μJ/cm² pulse centred at 535 nm. We deconvolve the fsTA map into two kinetics (c) and spectra (d) in a global analysis using the genetic algorithm. The kinetics were fit with a bi-exponential function to give a guide to the eye. We assign the spectra to the singlet (initial state) and excimer (subsequent state).[17]

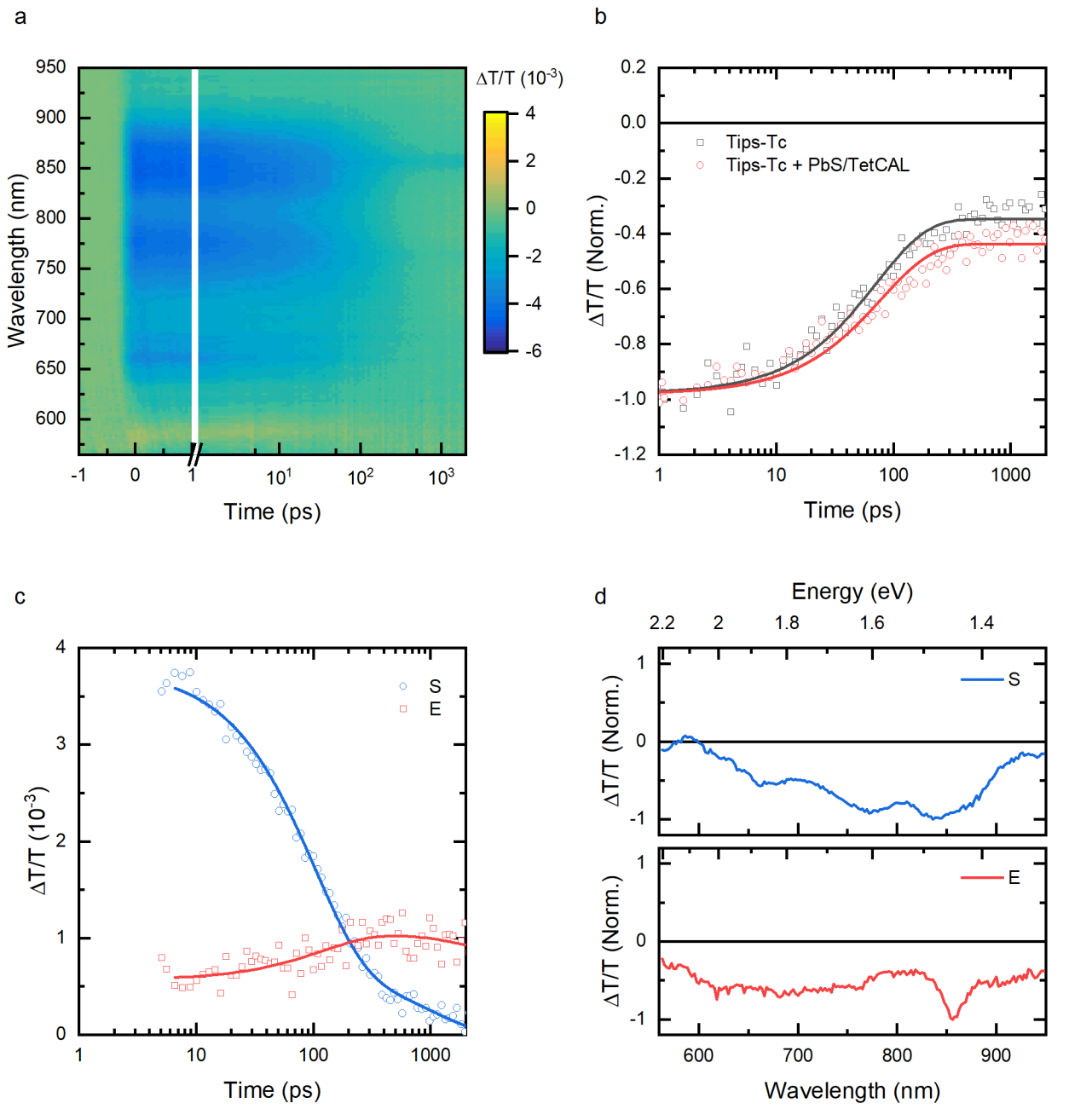

Figure S 11: a) Femtosecond transient absorption map of ~100 micron thick PbS/TetCAL (50 mg/mL) and TIPS-Tc (200 mg/mL) solution. The sample was excited with a 15 μJ/cm² pulse centred at 535 nm. b) Comparison of the signal strength at 860 nm between TIPS-Tc and PbS/TetCAL with TIPS-Tc. The kinetic fitting is achieved using a exponiential decay (capturing the singlet decay) with constant offset (residual signal due to the excimer state). We deconvolve the fsTA map into two kinetics (c) and spectra (d) in a global analysis using a genetic algorithm. The kinetics were fit with a bi-exponential function to give a guide to the eye. We assign the spectra to the singlet (initial state) and excimer (subsequent state).

Because of the strong absorption of the QDs, the probe pulse is significantly weaker in the TIPS-Tc + PbS/TetCAL solution at shorter wavelengths. This results in worse probe statistics at wavelengths below 700 nm compared with spectra of TIPS-Tc on its own. As a result, the spectral features like the TIPS-Tc's singlet stimulated emission (580 nm) and PIA (650 nm) appearing weaker as they have been masked noise. However, the Singlet and Excimer features in the range 700-950 nm are still clear and allow for spectral deconvolution of the two species.

	Time Constant (ps)
Solution	Singlet PIA Decay
Tips-Tc	71 ± 4
Tips-Tc + PbS/TetCAL	78 ± 6

Tabel S 4: Femtosecond transient absorption measured decay rate of the TIPS-Tc singlet state. Decay rate obtained by fitting an exponential decay with offset to the fsTA kinetics at 860 nm. Samples excited with 535 nm, fs pulses at 15 μJ/cm².

8.1.1 Singlet Energy Transfer

The TIPS-Tc singlet decay rate for solutions of TIPS-Tc and TIPS-Tc + PbS/TetCAL is given respectively by,

$$k_1 = k_{S_r} + k_{S_{nr}} + k_{EF}S_0 \,,$$

$$k_2 = k_{S_r} + k_{S_{nr}} + k_{EF}S_0 + k_{SET} \,.$$

The efficiency of singlet energy transfer is given by,

$$\eta_{SET} = \frac{k_{SET}}{k_{S_r}+k_{S_{nr}}+k_{EF}S_0+k_{SET}} = \frac{k_2-k_1}{k_2},$$

with uncertainty $\Delta\eta_{SET} = \left(\frac{k_1}{k_2}\right)\left(\frac{\Delta k_1}{k_1} + \frac{\Delta k_1}{k_1}\right)$. From the fitted fsTA TIPS-Tc singlet decay rates we find, $k_1 = 14.1 \pm 0.8\, ns^{-1}$ and $k_2 = 12.8 \pm 1.0\, ns^{-1}$. Therefore the efficiency of SET in a solution of TIPS-Tc (200 mg/mL) and PbS/TetCAL (50 mg/mL) is $\eta_{SET} = -0.10 \pm 0.15$. Putting the upper bound on the singlet transfer efficiency at 5% in this solution.

We observe a change in fsTA spectra that can be deconvolved by the genetic algorithm, to give spectra and kinetics that agree with the formation of an subsequent excimer/triplet state with a ~100 ps time scale. After the singlet decays the subsequent spectrum with PIA peak at 850 nm, is present at similar signal strengths, as observed from the genetic algorithm's deconvolution and the raw TA signal at times after 200 ps in figure S11b, indicating that singlet fission is still occurring with similar yields with the PbS/TetCAL QDs present. The insignificant change in singlet decay rate and similar intensities of the subsequent PIA spectrum, with and without the Pbs/TetCAL, indicates that there is no effect on the singlet fission process.

Additionally we note that no spectral feature in the 550-950 nm range were assigned to changes in the population of excited QD states. There is no sub 2 ns transfer to the QD, and so any population that the QD have before 2 ns is a result of direct photo excitation.

8.2 Nanosecond Transient Absorption

8.2.1 TIPS-Tc Fluence Dependence

The decay of TIPS-Tc triplet density after generation by singlet fission can be expressed as,[20]

$$\frac{d[T]}{dt} = -k_1[T] - k_2[T]^2 \,.$$

The strength of the measured TIPS-Tc triplet photo induced absorption at 840-850 nm is proportional to the total number of triplets present, $\frac{\Delta T}{T} \propto \int_V [T]\, dV$. We assume a uniform triplet density in the volume of integration described by the area and the penetration depth of the pump beam. This results in a linear

relationship between the measured triplet PIA strength and the TIPS-Tc triplet density, $\frac{\Delta T}{T} = \chi[T]$. Thus we find,

$$\frac{d(\Delta T/T)}{dt} = -k_1(\Delta T/T) - k'_2(\Delta T/T)^2 ,$$

where $k'_2 = k_2/\chi$. We find χ by measurement of the pump beam area and power, singlet fission yield (135%) and absorbance of TIPS-Tc (giving the 535 nm laser penetration depth). The analytical solution to this differential equation is,

$$\left(\frac{\Delta T}{T}\right)(t) = \left(\frac{\Delta T}{T}\right)_0 \frac{1-\beta}{\exp(k_1 t) - \beta},$$

with $\beta = \alpha/(k_1 + \alpha)$, and $\alpha = k'_2 \left(\frac{\Delta T}{T}\right)_0$. Using globing fitting of this analytical function, to multiple triplet decay kinetics at a range of fluences allows determination of the mono and bi-molecular decay rates (Figure S12 and Table S5). From the decay rates the fraction of triplets that decay mono-molecularly, f_1, and bi-molecularly, f_2, can be found using the following,[20]

$$f_1 = \frac{\beta - 1}{\beta}\ln(1-\beta) ,$$

$$f_2 = 1 - f_1 = 1 - \frac{\beta - 1}{\beta}\ln(1-\beta) ,$$

We find that at the pump fluences achievable in this nsTA experiment, the fraction of triplet decaying bi-molecularly is between 0.5 – 1, within uncertainty (Table S5). Most triplets are decaying bi-molecularly even at the lowest measurable fluences.

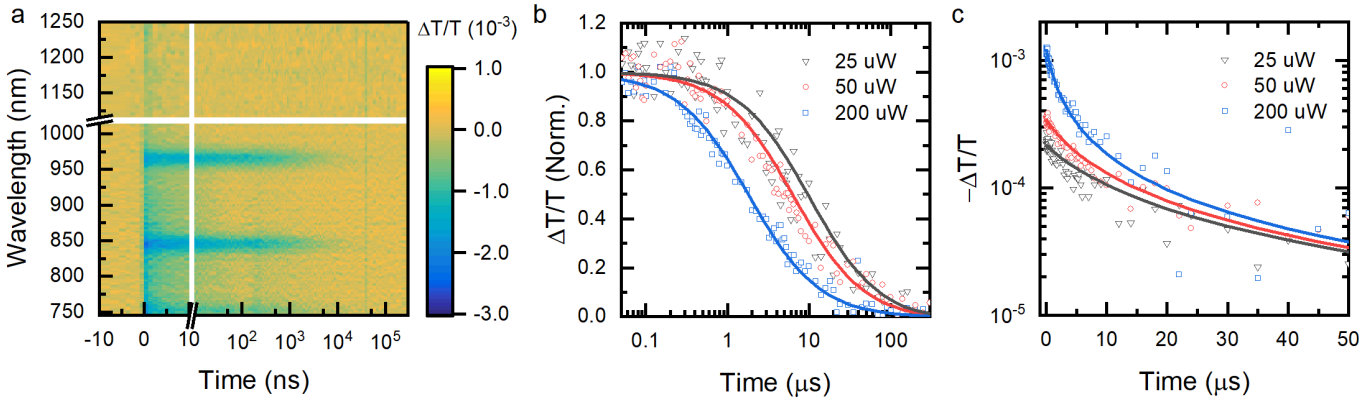

Figure S 12: a) Nanosecond transient absorption map of ~100 micron thick TIPS-Tc solution (200 mg/mL). The sample was excited with a 168 μJ/cm² pulse centred at 535 nm. The normalised (b) and raw (c) nsTA signal strength at 840-850 nm for fluences from 25-200 μW (21-168 μJ/cm²). Kinetics were fitted globally with an analytical function for a bi-molecular decay process.

Power (μW)	Pulse Power (μJ/cm²)	k_1 (1/ms)	k'_2 ((ΔT/T)$^{-1}$ ns^{-1})	ΔT/T (0)	[T] (1/cm³)	k_2 (cm³/ns)	f2
25	21	5.6 ± 5.1	0.44 ± 0.02	2.2E-4 ± 5.8E-6	0.9E18	7.6E-23 ± 0.3E-23	0.83 ± 0.36
50	42	5.6 ± 5.1	0.44 ± 0.02	3.4E-4 ± 6.3E-6	1.8E18	7.6E-23 ± 0.3E-23	0.88 ± 0.34
200	168	5.6 ± 5.1	0.44 ± 0.02	1.2E-3 ± 9.7E-6	7.2E18	7.6E-23 ± 0.3E-23	0.95 ± 0.35

Tabel S 5: Nanosecond transient absorption fitting parameters for the TIPS-Tc triplet PIA (840-850 nm) of TIPS-Tc at 200 mg/mL. Transient absorption bi-molecular decay rates are converted to triplet density bi-molecular decay rates by estimation of the initial triplet density.

8.2.2 QD Transient Absorption

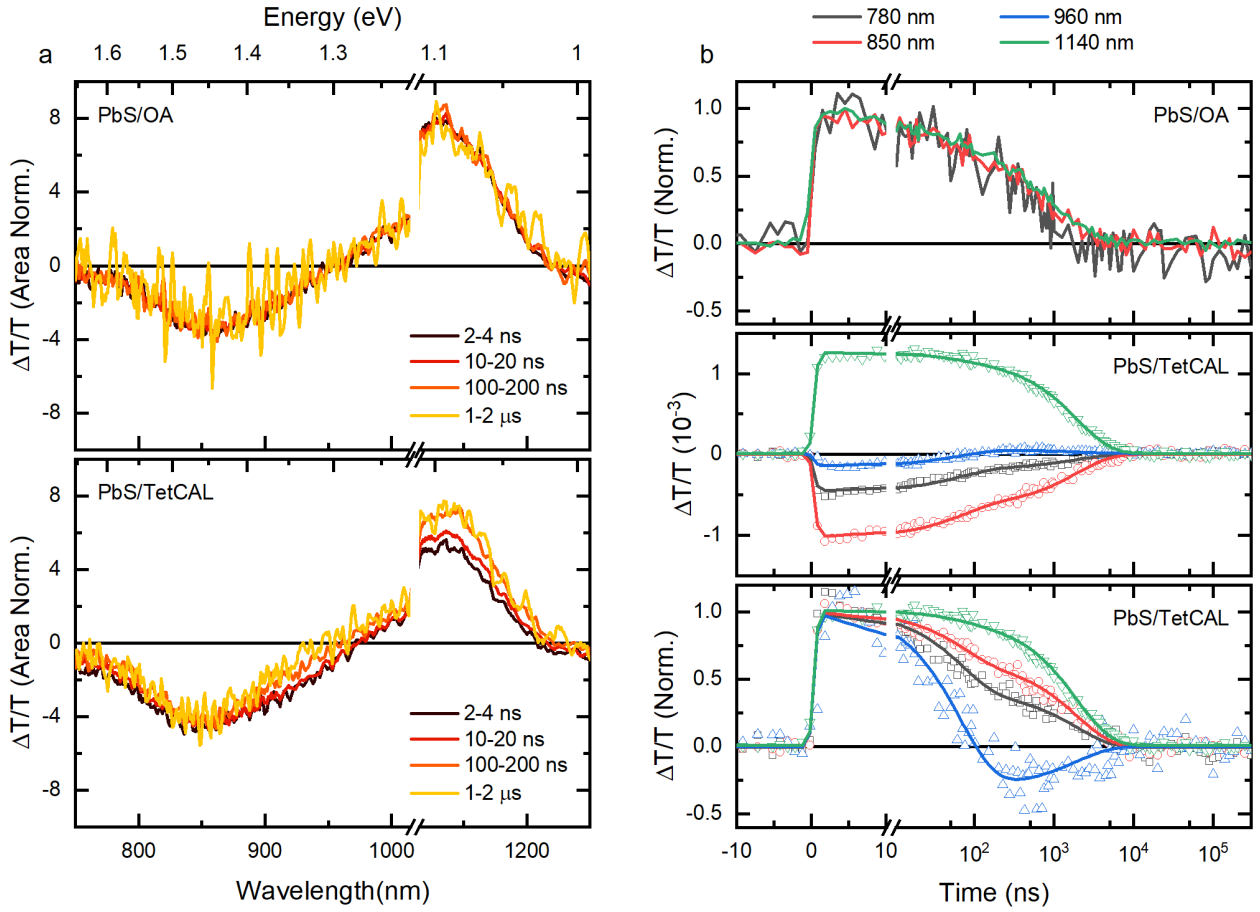

Figure S 13: a) Average nanosecond transient absorption spectra for ~100 micron thick PbS/OA and PbS/TetCAL solutions (10 mg/mL). The samples were excited with a 42 μJ/cm² pulse centred at 535 nm. b) corresponding transient absorption kinetics across the probe range. The PbS/TetCAL kinetics were fit with bi-exponential functions.

The time constant extracted by global fitting for the decay of the PbS/TetCAL GSB is 1900 ± 40 ns. In agreement with the IR TCSPC measurement for the IR photoluminescence lifetime of PbS/TetCAL. The time constant extracted for the additional PIA feature that we observe when exciting PbS/TetCAL at 535 nm is 68 ± 5 ns. We assign this to a PIA present due to excitation on the TetCAL because of direct excitation from the pump pulse.

8.2.3 QD Concentration Dependence

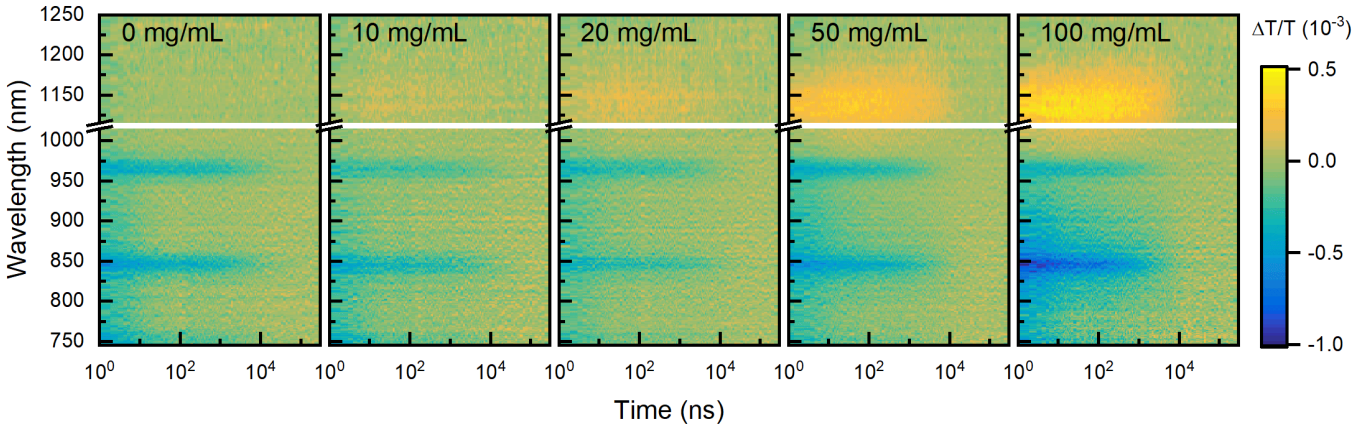

Figure S 14: Nanosecond transient absorption maps for solutions of concentrated TIPS-Tc (200 mg/mL), with varying concentrations of PbS/TetCAL QDs (0-100 mg/mL), with a 535 nm pump at 50 µW (42 µJ/cm²).

The presence of long lived triplet PIA features at 850 and 980 nm in solutions of TIPS-Tc + PbS/TetCAL at QD concentration from 0 – 100 mg/mL is further indication that singlet fission continues as normal under the addition of the QDs.

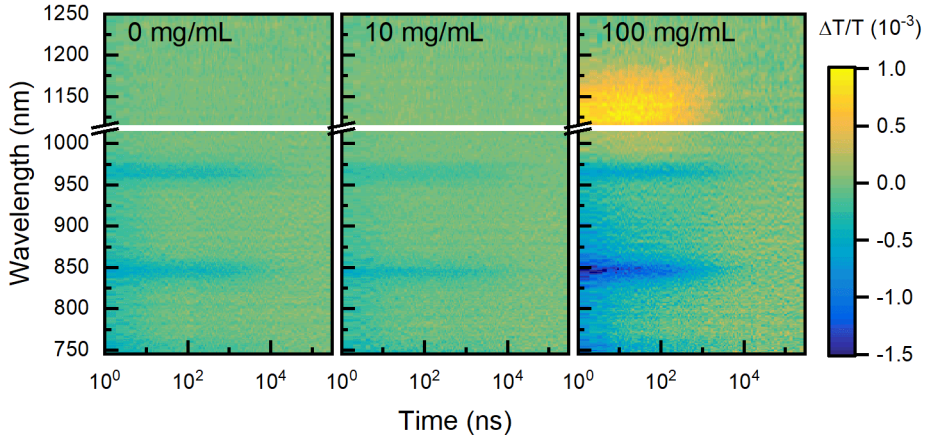

Figure S 15: Nanosecond transient absorption maps for solutions of concentrated TIPS-Tc (200 mg/mL), with varying concentrations of PbS/OA QDs (0-100 mg/mL), with a 535 nm pump at 50 µW (42 µJ/cm²).

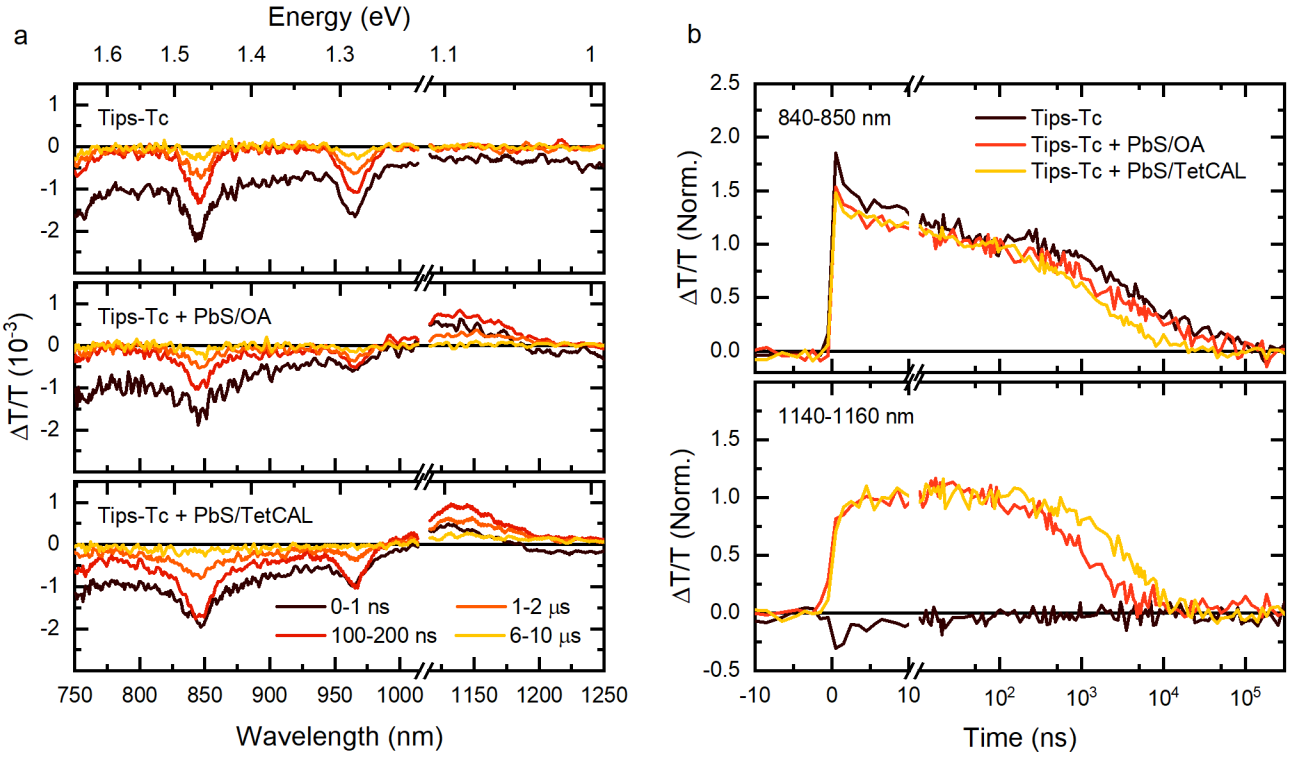

Figure S 16: a) Average nanosecond transient absorption spectra for ~100 micron thick TIPS-Tc (200 mg/mL), PbS/OA (100 mg/mL) with TIPS-Tc (200 mg/mL) and PbS/TetCAL (100 mg/mL) with TIPS-Tc (200 mg/mL) solutions. The samples were excited with a 168 μJ/cm² pulse centred at 535 nm. b) Normalised average nanosecond transient absorption kinetics at the TIPS-Tc triplet PIA (840-850 nm) and the PbS QD GSB (1140-1160 nm). The samples were excited with a 42 μJ/cm² pulse centred at 535 nm.

Comparison of the transient absorption spectra and kinetics for TIPS-Tc by itself along with PbS/OA and PbS/TetCAL QDs, with a 535 nm pump at 50 μW (42 μJ/cm^2). The key features to note are the reduced lifetime of the TIPS-Tc triplet PIA feature at 840-850 nm due to quenching from the PbS/TetCAL QDs and the increased apparent lifetime of the PbS/TetCAL relative to the PbS/OA QDs due to transfer from the TIPS-Tc triplets.

8.2.4 Removal of Initial QD Population

Earlier we showed that there is no transfer to the QDs within the first 2 ns. Here we extend that range to claim that there is no significant difference in the QD dynamics within the first 100 ns with or without the TIPS-Tc present (Figure S17). Therefore the initial TA signals showing QD features before 100 ns are due to direct photo excitation.

To identify the transfer of excitons from the triplet state of the TIPS-Tc to the PbS/TetCAL QDs, we take the difference of the transient absorption maps for the TIPS-Tc +PbS/TetCAL mixtures relative to the PbS/TetCAL QDs on their own. To do this we assume that any QD GSB that is present initially (but after the singlet PIA in the same region has decayed) is due to direct excitation from the 535 nm pump and thus will have a transient absorption map that is identical to the PbS/TetCAL under 535 nm excitation on its own, and can be removed from the transient absorption data of interest. To find this initial population of QDs that are directly excited we take the QD GSB kinetics averaged in the region 1120-1160 nm for the QDs on their own and scale it such that the value in the range 20-40 ns agrees with the GSB signal in the mixtures (Figure S17a). This method assumes that no excitations are transferred before 20 ns, however this can be justified since the triplet signatures do not decay significantly even after 100 ns and so no significant amount of triplet excitons could have transferred before this time (Figure S16b).

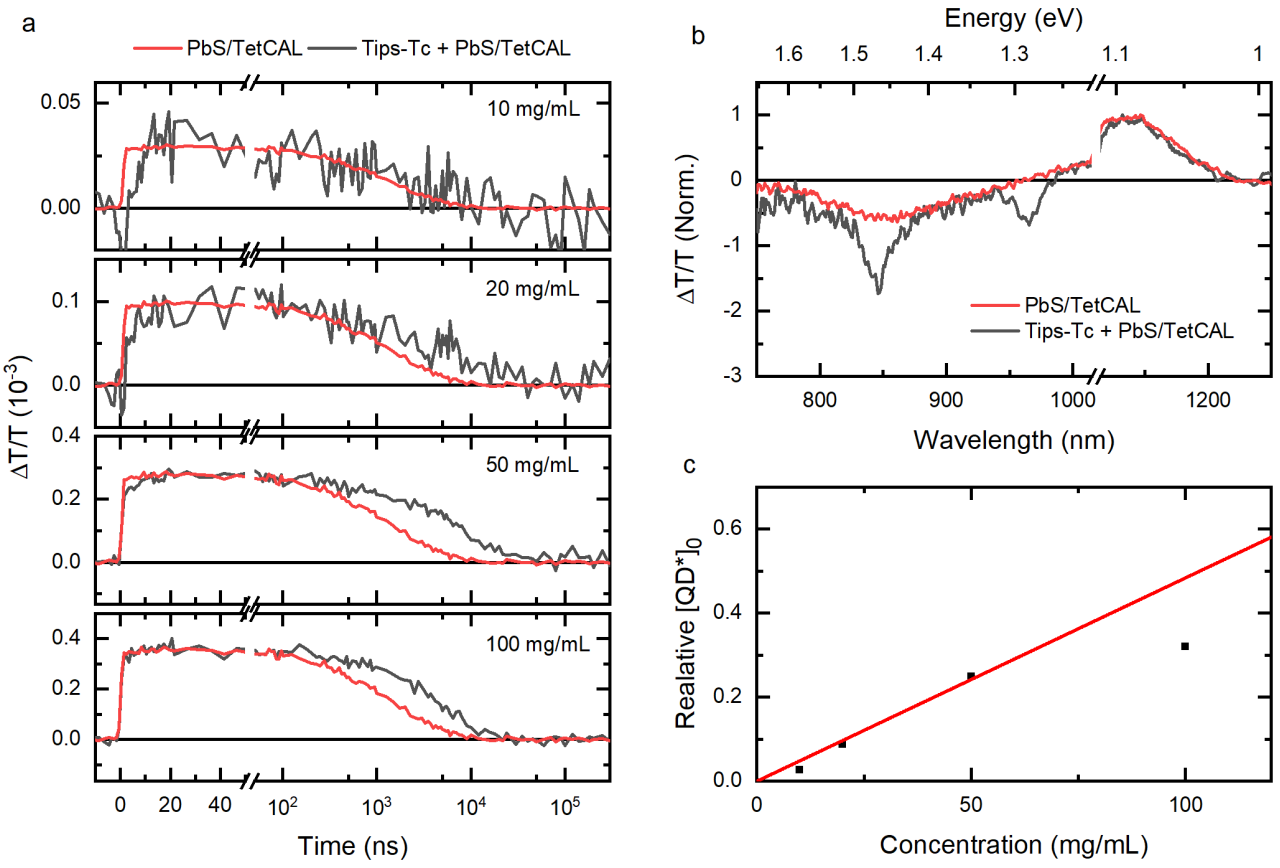

Figure S 17: a) Nanosecond transient absorption kinetics at 1140-1160 nm for solutions of TIPS-Tc (200 mg/mL) and PbS/TetCAL at varying concentrations under 42 μJ/cm² 535 nm excitation (black curves). Subsequently, the 1140-1160 nm kinetic for PbS/TetCAL alone(10 mg/mL), under the same excitation, is scaled such that they overlap during the time period 20-40 ns. b) Corresponding nanosecond transient absorption spectra for PbS/TetCAL (10 mg/mL) and PbS/TetCAl (100 mg/mL) with TIPS-Tc (200 mg/mL), averaged over 100-200 ns and normalised to the QD's GSB strength. The difference between the two spectra matches the spectral features of the TIPS-Tc triplet spectrum, indicating that at this time the only species present are the excited QD state and the TIPS-Tc triplet state. c) The scaling factors used to overlay the PbS/TetCAL GSB signal with the signal present in the solution SF-PM samples. A linear function was fit to the scaling factors for concentrations from 10-50 mg/mL. The 100 mg/mL data point appears to be an outliner to this linear

fit. This is possibly due to variation in the probe-pump overlap between measurements, resulting in a lower measured signal than expected.

8.2.5 Transient Absorption Difference Maps

The scaling factors obtained previously are used to calculate the full difference maps between TIPS-Tc + PbS/TetCAL and PbS/TetCAL, under 535 nm excitation (Figure S18).

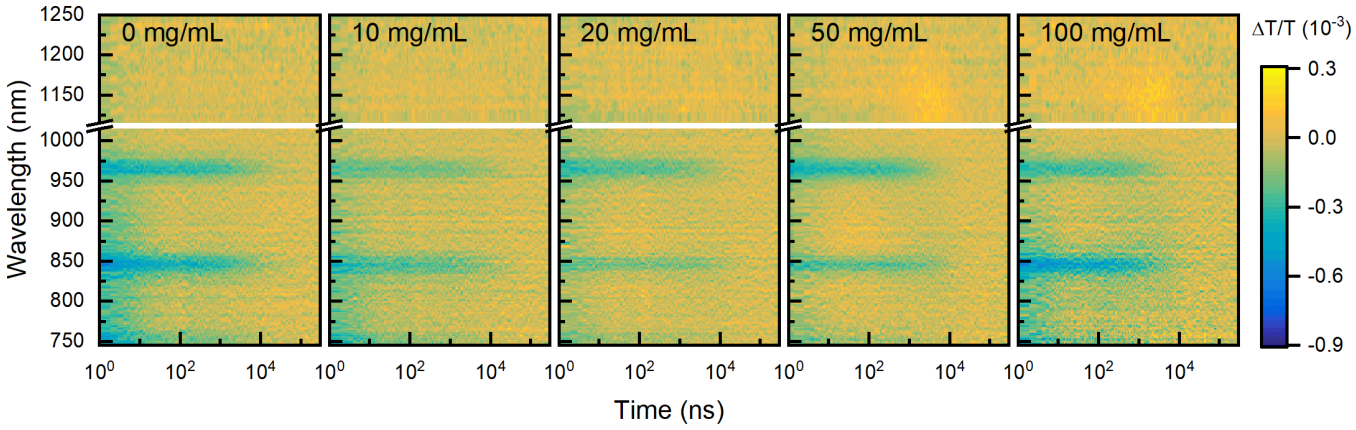

Figure S 18: Nanosecond transient absorption difference maps (relative to PbS/TetCAL QDs) for solutions of concentrated TIPS-Tc (200 mg/mL), with varying concentrations of PbS/TetCAL QDs (0-100 mg/mL), with a 535 nm pump at 42 µJ/cm².

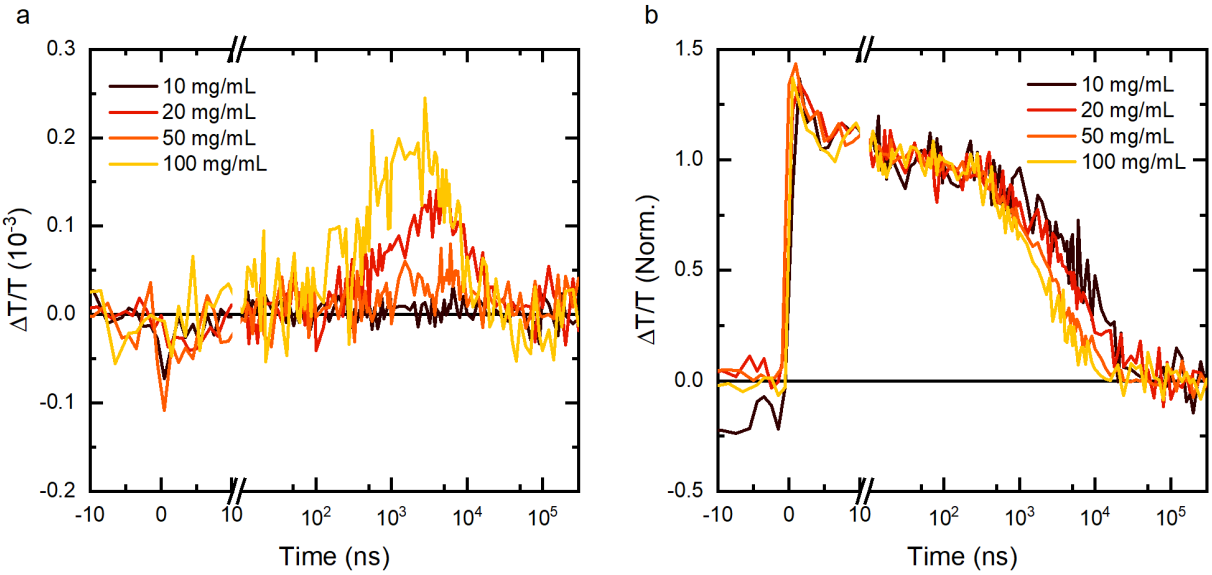

Figure S 19: Nanosecond transient absorption difference kinetics at the PbS QD GSB, 1140-1160 nm (a) and TIPS-Tc triplet PIA 860-850 nm (b) (relative PbS/TetCAL QDs) for solutions of concentrated TIPS-Tc (200 mg/mL), with varying concentrations of PbS/TetCAL QDs (10-100 mg/mL), with a 535 nm pump at 42 µJ/cm².

8.2.6 Triplet Quenching

Using linear regression the kinetics of the TIPS-Tc triplet were isolated from the signatures of the other species, for the TIPS-Tc + PbS/TetCAL solutions. This was done using transient absorption spectra for the TIPS-Tc triplet (1 µs spectrum, just TIPS-Tc), singlet/excimer (from fitting the remain spectral component in the TIPS-Tc TA map, in the genetic algorithm with the triplet spectrum as a reference) and PbS/TetCAL excited QD state

(400 ns spectrum, PbS/TetCAL, 535 nm excitation), to reconstruct the observed transient absorption maps via linear regression, solving for the kinetics associated with these spectra (Figure S20a).

We approximate the triplet bi-molecular decay rate as constant with respect to changes in the QD concentration. This relies on the QDs having little effect on the volume which the triplets occupy and the triplet diffusion constant. Using the bi-molecular rate constant calculated from TIPS-Tc under 535 nm excitation (Table S5), we apple a global fit to the decay of the triplet population for PbS/TetCAL QD concentration from 0-100 mg/mL (Figure S20b). This allows us to extraction of the mono-molecular decay rate as a function of QD concentration. Following a Stern-Volmer like analysis, where the rate of transfer is proportional to the concentration of QDs in the ground state (equivalent to the concentration of QDs in this case as we are in a low excitation regime) (Figure S20c). This allows fitting of the following function,

$$k_1 = k_T + k_{TET}[QD]_0 \, .$$

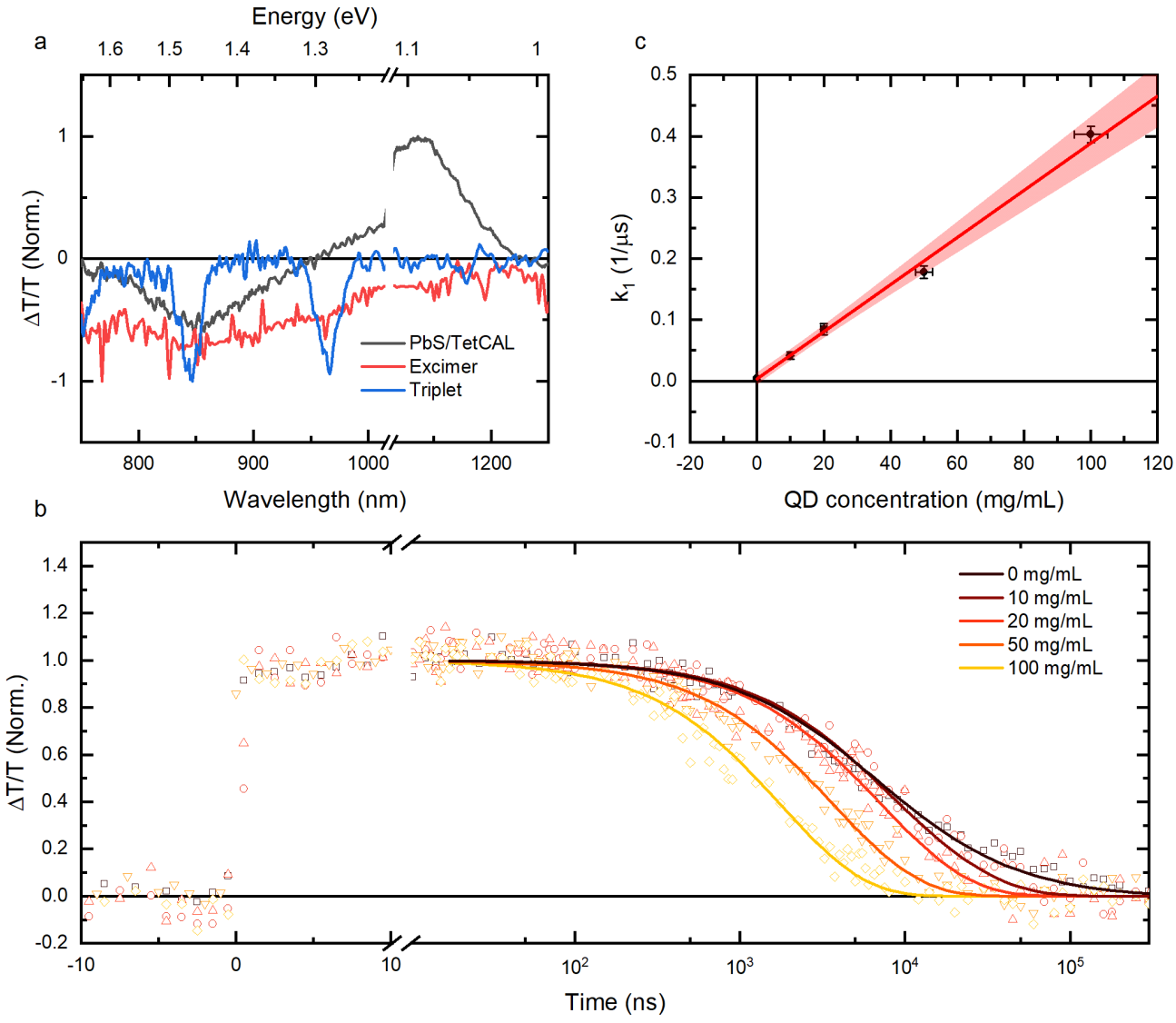

Figure S 20:Normalised nanosecond transient absorption spectra used to deconvolve the TIPS-Tc with PbS/TetCAL nanosecond transient absorbed difference maps. The PbS/TetCAL spectrum (black) is the spectrum 100-200 ns after 535 nm excitation. The excimer (red) and triplet (blue) spectra were obtained via global analysis using the genetic algorithm on nanosecond transient absorption of TIPS-Tc (200 mg/mL) under 535 nm pulsed excitation. b) Normalised triplet spectral component from deconvolution via linear regression for PbS/TetCAL QD concentratiosn from 0 to 100 mg/mL, 42 μJ/cm² excitation. Triplet decay kinetics were fitted globally with an analytical

function for a bi-molecular decay process. The bi-molecular decay rate was fixed as the value obtained for TIPS-Tc on its own and the mono-molecular rate to varying between samples. c) The obtained mono-molecular TIPS-Tc triplet decay rate as a function of PbS/TetCAL QD concentration (black dots), with error bars representing 95% confidence bounds from fitting of the triplet decay kinetics. The relationship between mono-molecular TIPS-Tc triplet decay and PbS/TetCAL QD concentration is in agreement with a linear fit (red line, 95% confidence bound represented as the red shaded region) with slope 0.0039 ± 0.0001 $(mg/mL)^{-1}\mu s^{-1}$ and intercept 0.0035 ± 0.0032 μs^{-1}.

From previous diffusivity measurements and estimates of the interaction distance and the molar mass of the QD we predict a bi-molecular transfer rate of 0.085 $(mg/mL)^{-1}$ μs^{-1}, which is higher than the 0.0039 ± 0.0001 $(mg/mL)^{-1}$ μs^{-1} ($5.1x10^{8} \pm 0.1x10^{8}$ M^{-1} s^{-1}) obtained from the quenching of the triplet PIA. However, the data is well described by a Stern-Volmer-like quenching, indicating the transfer is diffusion limited. This indicates that not every collision between a triplet exciton on a TIPS-Tc molecule and the surface of the PbS/TetCAL QD is resulting in a successful triplet transfer event. Possible explanations for this include non-uniform coverage of the TetCAL ligand over the surface of the PbS QD or residual OA ligands inducing steric hindrance.

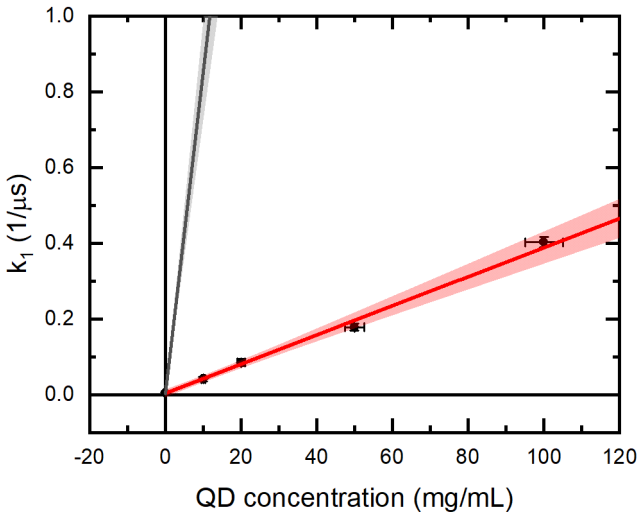

Figure S 21: Measured TIPS-Tc triplet decay rate as a function of PbS/TetCAL QD concentration, with error bars representing 95% confidence bounds from fitting of the triplet decay kinetics (black dots) and a linear fit (red line). Predicted triplet decay rate due to PbS/TetCAL and TIPS-Tc diffusion limited bi-molecular interaction rate, as calculated in section 6.

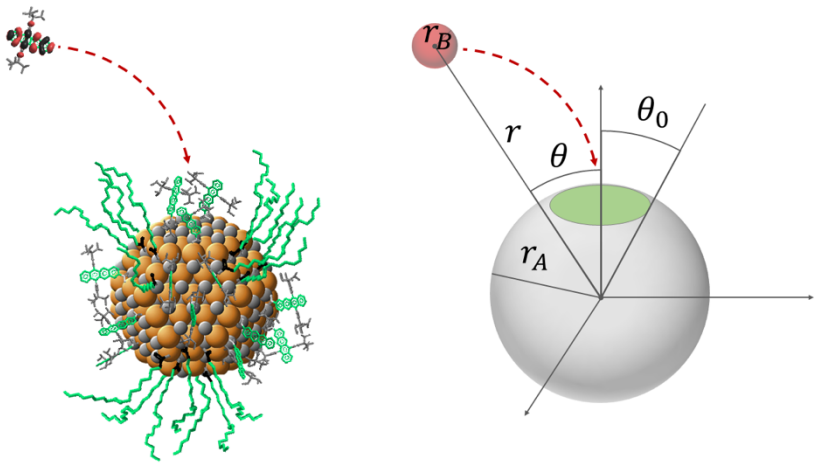

Figure S 22: Illustration showing the possibly non-uniform coverage of TetCAL and OA ligands surrounding the PbS QD (left). Any remaining OA ligands attached to the surface of the PbS QD may sterically hinder the interaction between free TIPS-Tc molecules in

solution and the TetCAL ligand attached to the PbS QD. Analogous model where only interaction events with attack angle θ less than θ_0 collide with the active surface area (green).

8.2.7 Analysis of Triplet Decay Parameterisation

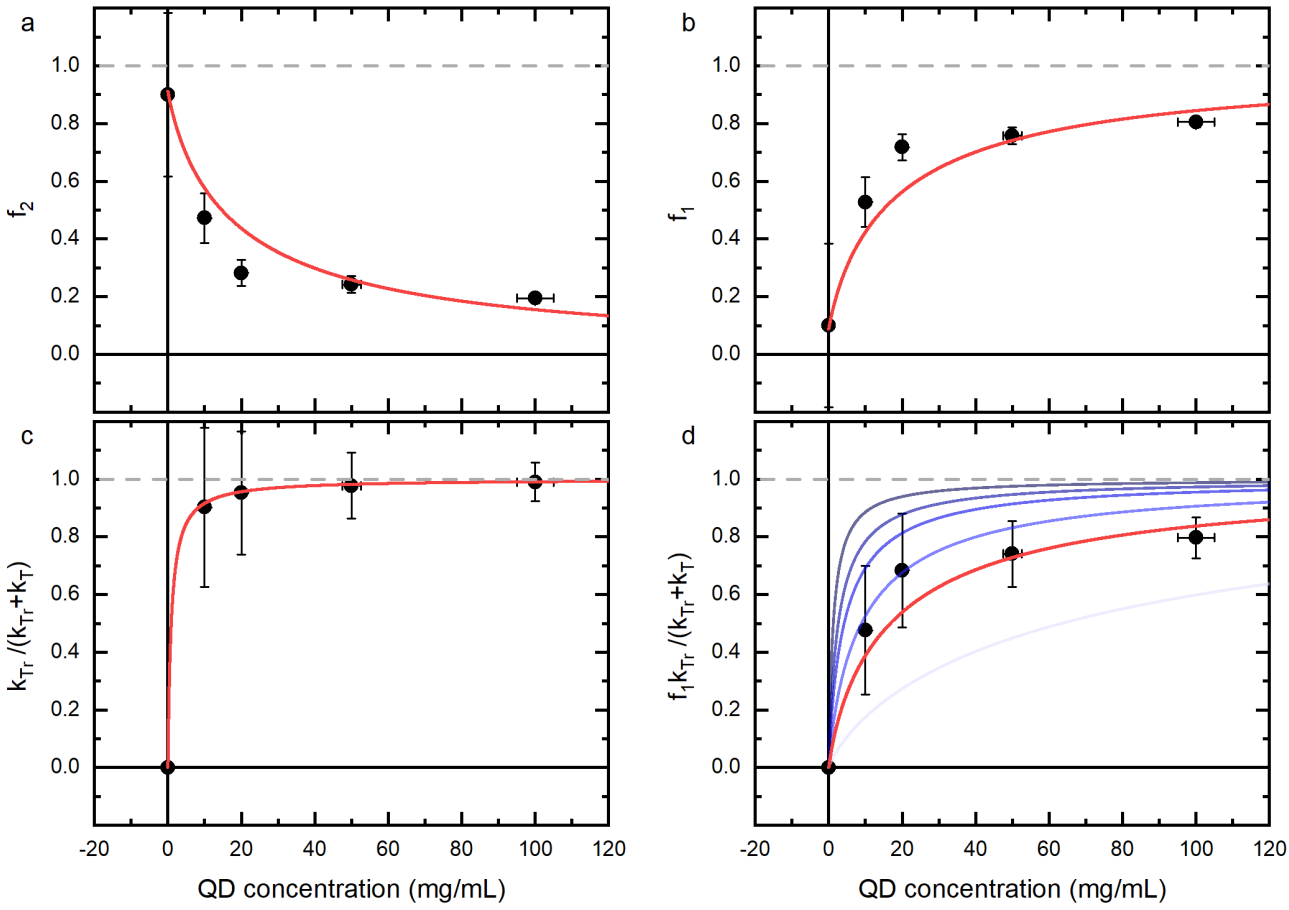

Figure S 23: Nanosecond transient absorption fitting parameters for the TIPS-Tc triplet PIA (840-850 nm) of TIPS-Tc (200 mg/mL) and varying concentrations of PbS/TetCAL QDs (0-100 mg/mL), excited at 535 nm with 42 μJ/cm² (50 μW). (black circles) The fraction of TIPS-Tc triplet excitons that decay bi-molecularly (a), mono-molecularly (b), mono-molecular branching ratio (c) and fraction of triplet excitons that are quenched by transfer to the PbS/TetCAL QDs (d), as functions of PbS/TetCAL QD concentration. Error bars are calculated via propagation of uncertainties arising from the 95% confidence bounds for the fitted parameters. From the bi-molecular TIPS-Tc triplet and PbS/TetCAL QD transfer rate, 0.0039 ± 0.0001 (mg/mL)$^{-1}$μs^{-1}, we calculate the same parameters in a-d, as continuous functions of the QD concentration, for the pump power used in the nanosecond transient absorption experiment (50 μW) (red lines). Using the obtained triplet transfer and decay parameters we simulate the fraction of triplet excitons that are quenched by transfer to the PbS/TetCAL QDs as functions of PbS/TetCAL QD concentration, for pump powers 1, 5, 10, 25, 200 μW (dark to light blue lines). Transient absorption signals at these lower pump powers are beyond our current experimentally reachable signal-to-noise. At simulated, low pump powers, the fraction of triplets transferred to the PbS/TetCAL QDs trends to 100%, for a QD concentration of 50 mg/mL.

From the obtained TIPS-Tc triplet transfer and decay parameters, along with the intrinsic PbS/TetCAL QD excited state lifetime, we have all parameters for the differential equations that describe the triplet and QD time-dependent populations after singlet fission,

$$\frac{dT_1}{dt} = -(k_T + k_{TET}X_0)T_1 - k_2T_1^2 \,,$$

$$\frac{dX_1}{dt} = k_{TET}X_0T_1 - k_XX_1 \,.$$

The equation for the triplet population has an analytical solution as described earlier. This solution for $T_1(t)$ can be substituted into the differential equation for the QD population. There exists an analytical solution to the aforementioned differential equation in terms of hypergeometric functions. However, to avoid the complexities of dealing with these intricate functions, we solve for the time-dependent QD population using numerical techniques. To illustrate the effect of bi-molecular TIPS-Tc triplet decay we simulate the triplet and QD populations with and without bi-molecular decay (figure S24 a and b).

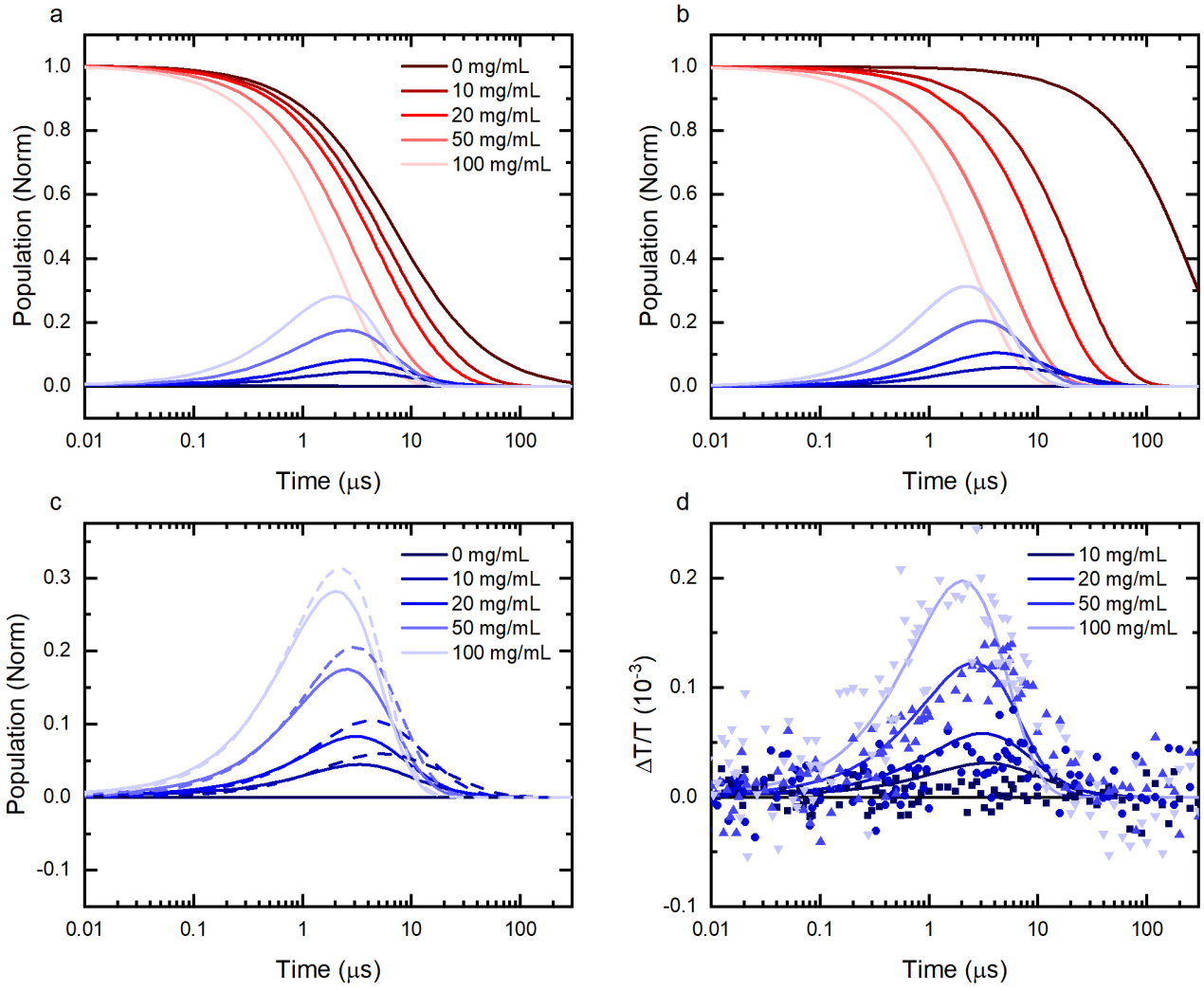

Figure S 24: Simulation of the triplet (red) and QD populations (blue) with and without bi-molecular decay (a and b) for varying concentration of PbS/TetCAL QDs. Simulated populations are calculated using the experimentally obtained kinetic parameters and

excitation of 535 nm 42 µJ/cm². c) Comparison of the predicted QD population with (solid lines) and without (dashed lines) triplet bi-molecular decay. d) Predicted QD populations (with all parameters included) scaled to overlay with the measured nanosecond transient absorption difference kinetics at the PbS/TetCAL QD GSB (1140-1160 nm).

Fluence dependence for the difference kinetics for TIPS-Tc (200 mg/mL) + PbS/TetCAL (100 mg/mL). The higher QD population at higher fluence is observed as expected. Along with a fast triplet decay due to increased bi-molecular decay. Simulated QD population for the 200 µW pump pumper relative to the lower 50 µW pump power is in reasonable agreement with the observed dot GSB data in A. However the simulated triplet population for the 200 µW kinetic does not decay as rapidly as the measured TA kinetic. This could indicate that the TIPS-Tc triplet bi-molecular recombination rate is higher in samples with high QD loading compared to TiPS-Tc on its own.

As expected a higher pump fluence results in a higher QD population, along with a faster triplet decay due to increased bi-molecular decay (Figure S25 a and b). Simulated population dynamics for the 200 µW pump pumper relative to the lower 50 µW pump power is in reasonable agreement with the observed dynamics (Figure S25 c and b). However, the simulated triplet population for the 200 µW kinetic does not decay as rapidly as the measured TA kinetic.

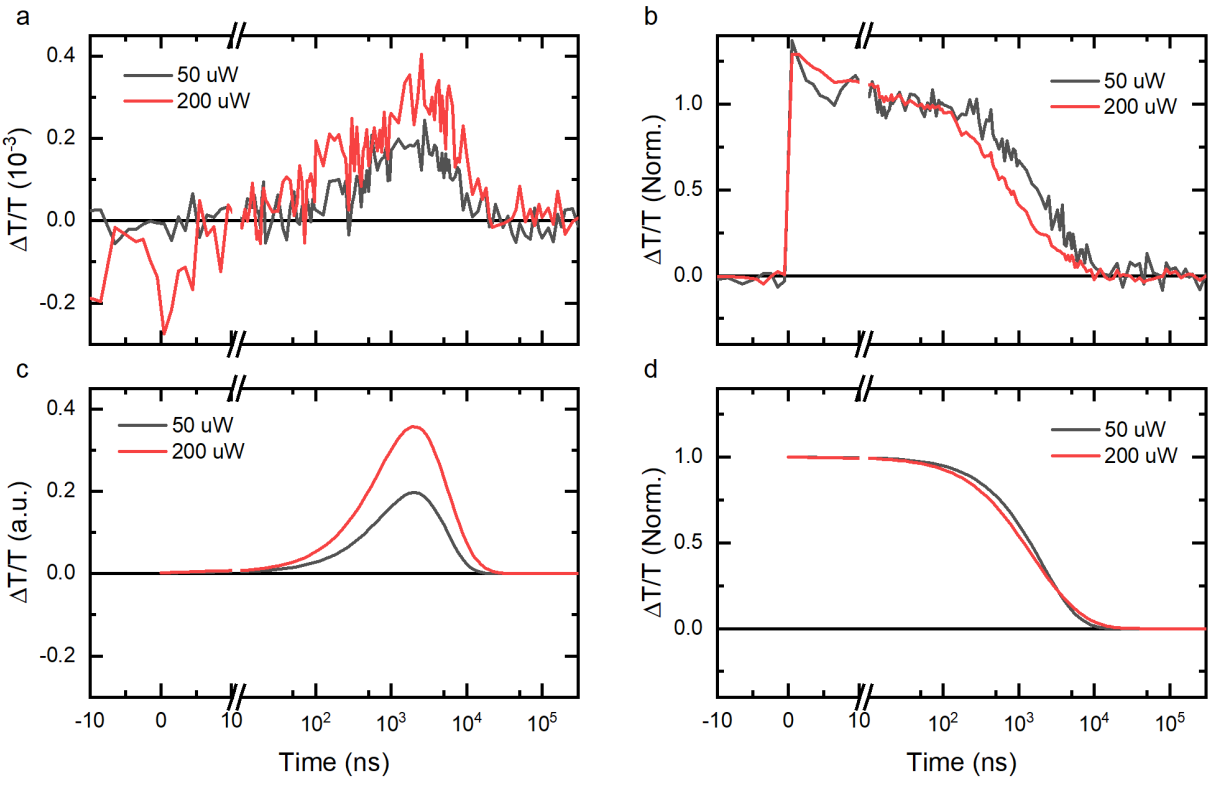

Figure S 25: Fluence dependence for the nanosecond transient absorption difference kinetics for the PbS/TetCAL QD GSB (1140-1160 nm) (a) and TIPS-Tc triplet PIA (840-850 nm) for TIPS-Tc (200 mg/mL) with PbS/TetCAL (100 mg/mL) excited at 42 (black) and 168 (red) µJ/cm². The corresponding simulated QD (c) and triplet (d) populations.

9 Solar- Equivalent Fluence

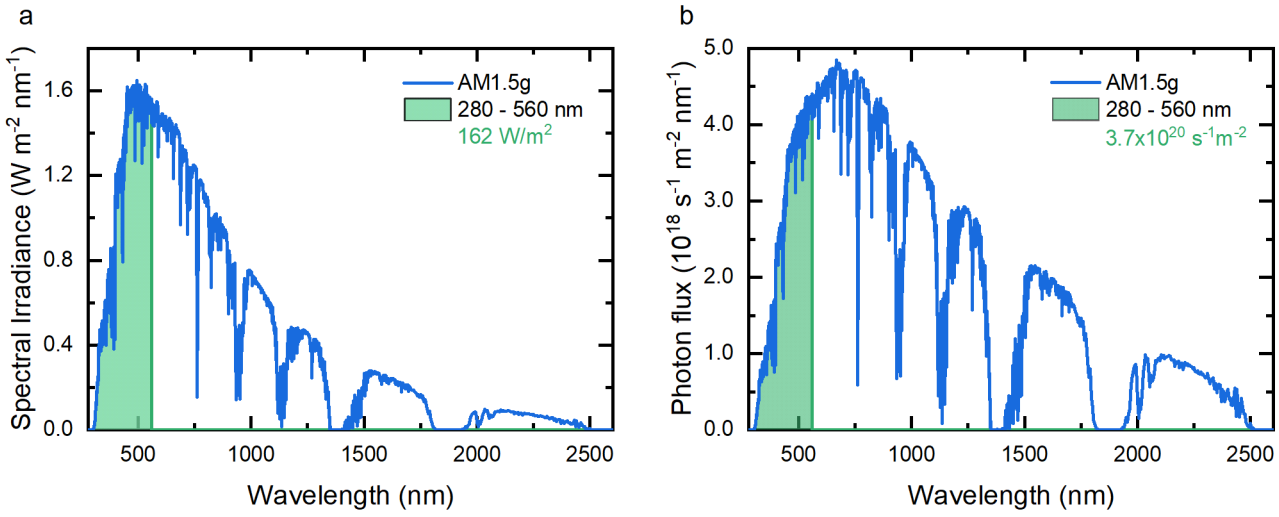

Figure S 26: Calculation of the available spectral irradiance and photon flux from the far UV (280 nm) to the absorption tail of TIPS-Tc (560 nm). a) The spectral irradiance of the AM1.5g solar spectrum, with the available solar flux calculated by the integration from the range 280 – 560 nm. b) The solar photon flux, with the available photon flux calculated by the integration from the range 280 – 560 nm.

For comparison to steady state PL measurements we calculate the laser fluence required, with 532 nm excitation, for an equivalent photon flux to that available (280-560 nm) under AM1.5g irradiance.[21] For the available photon flux of 3.67×10^{20} $s^{-1}m^{-2}$, the equivalent 532 nm laser fluence is 13700 µW/cm^2.

10 Steady State Modelling

Starting from the differential equation for the triplet population,

$$\frac{dT}{dt} = -(k_T + k_{TET})T - k_2T^2 + G\,,$$

where *G* is the rate of triplet generation from singlets undergoing singlet fission. After rearrangement under steady state conditions one arrives at the polynomial,

$$k_2T^2 + (k_T + k_{TET})T - G = 0\,.$$

Solving for positive *T* leads to,

$$T = -\frac{k_T + k_{TET}}{2k_2} + \sqrt{\left(\frac{k_T + k_{TET}}{2k_2}\right)^2 + \frac{G}{k_2}}\,.$$

The triplet transfer efficiency is given by $\eta_{TET} = \frac{k_{TET}T}{G}$. Substituting the above expression for T gives,

$$\eta_{TET} = \frac{k_{TET}}{G}\left(\sqrt{\left(\frac{k_T + k_{TET}}{2k_2}\right)^2 + \frac{G}{k_2}} - \frac{k_T + k_{TET}}{2k_2}\right).$$

Under steady state conditions the rate of IR PL emission from the solution SF-PM can be expressed as $PL_{QD} = \phi G\eta_{TET}\eta_{QD}$. Where ϕ represents the PL collection factor and η_{QD} is the QD PL efficiency. This expression can

be approximated in the regimes of low and high triplet generation rate as follows. When $G \ll \left(\frac{k_T+k_{TET}}{2k_2}\right)^2 k_2$, the IR PL from triplet transfer trends to,

$$PL_{QD} = \phi\eta_{QD}\frac{k_{TET}}{k_T + k_{TET}}G\,.$$

While at high triplet generation rates, $G \gg \left(\frac{k_T+k_{TET}}{2k_2}\right)^2 k_{TTA}$, the IR PL trends to,

$$PL_{QD} = \phi\eta_{QD}k_{TET}\sqrt{\frac{G}{k_2}}.$$

The intersection of these to regimes represents the threshold triplet generation and corresponding the incident photon flux, above which triplet exciton transfer and triplet monomolecular decay are no longer competitive with triplet bi-molecular decay. This threshold triplet generation rate, given by the intercept of the trends at low and high *G* is given by,

$$G_{Th} = \frac{(k_T + k_{TET})^2}{k_2}.$$

While the threshold photon absorption rate in the TIPS-Tc is given by $I_{Th} = G_{Th}/\eta_{sf}$. At the threshold generation rate G_{th}, the triplet transfer efficiency is given by,

$$\eta_{TET} = \left(\sqrt{\frac{5}{4}} - \frac{1}{2}\right) \times \frac{k_{TET}}{k_T + k_{TET}} = 0.618 \times \eta_{TET,0}\,.$$

Where $\eta_{TET,0}$ is the triplet transfer efficiency in the low G regime. This indicates that although G_{Th} is useful for indicating when bi-molecular processes are competitive with mono-molecular triplet decay process, it is not a useful criteria for solution SF-PM design. For example, a valuable criteria might be, what is the generation rate at which the triplet transfer efficiency is given $\eta_{TET} = \alpha \times \eta_{TET,0}$? In this case the α threshold generation rate is given by,

$$G_\alpha = \left(\frac{1-\alpha}{\alpha^2}\right) \times \frac{(k_T + k_{TET})^2}{k_2} = \left(\frac{1-\alpha}{\alpha^2}\right) \times G_{Th}\,.$$

However, this criteria does not grantee high performance of the SF-PM. Ideally what is required is a criteria at which the triplet exciton transfer efficiency is a given value β. The β generation rate for which this is true is given by,

$$G_\beta = \frac{k_{TET}^2}{k_2\beta}\left(1 - \beta\frac{k_T + k_{TET}}{k_{TET}}\right).$$

This gives a relationship between the QD concentration dependent triplet transfer rate, k_{TET}, and the maximum triplet generation rate, G_β, such that the triplet transfer efficiency is at least the fraction β.

Simulation of triplet transfer efficiencies under steady state conditions are calculated via the parameters extracted from the transient measurements for the bi-molecular decay of the TIPS-Tc triplets, under 535 nm excitation (Figures S27, S28 and S29).

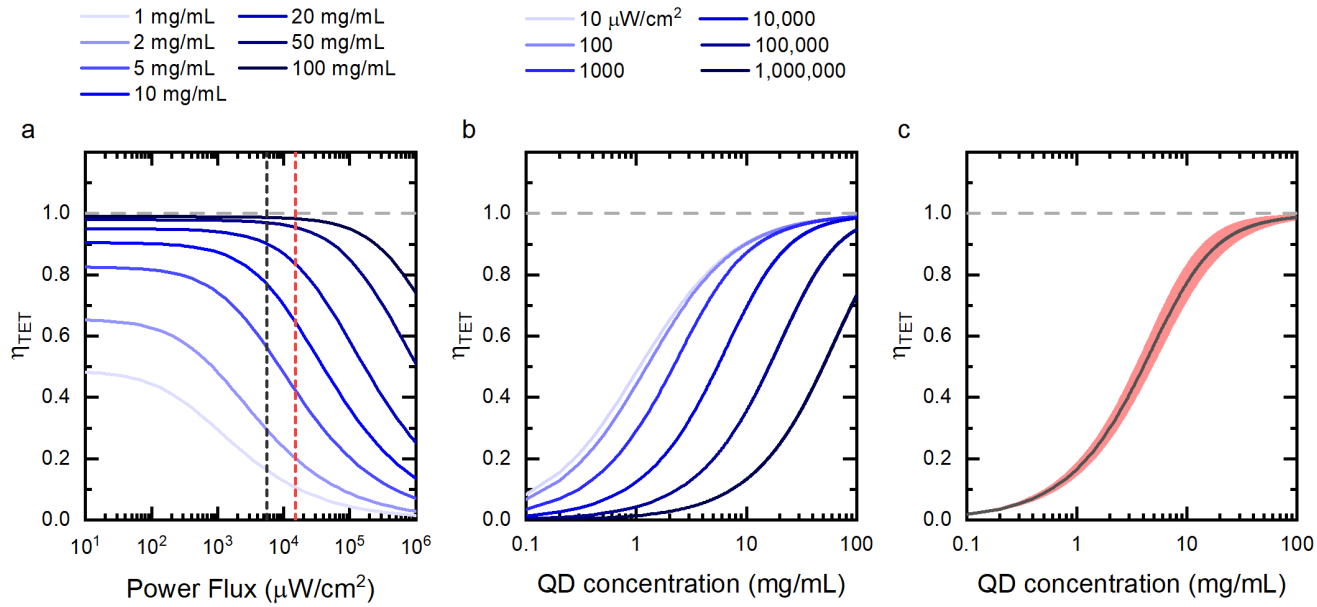

Figure S 27: Simulated triplet transfer efficiencies using the equations for the triplet transfer efficiency for various PbS/TetCAL QD concentrations (a) and incident fluences (b). The vertical dashed black line indicates the laser fluence used in the IR PLQE measurements (500 μW/cm²), while the red dashed line indicates the equivalent solar fluences (13.7 mW/cm²). c) Predicted triplet transfer efficiency at the photon flux used for the IR PLQE measurements, using the extracted triplet transfer and decay rates. The shaded region represents the uncertainty in the triplet transfer efficiency based on propagation of uncertainties form the triplet decay rates.

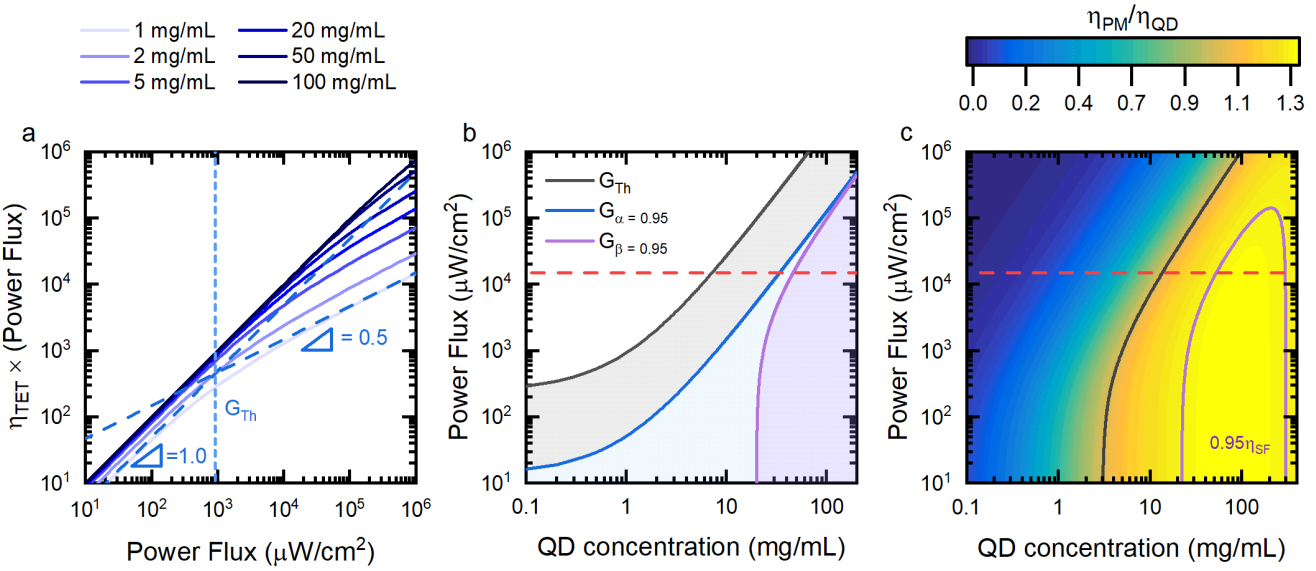

Figure S 28: Simulated steady state SF-PM response. a) Simulated steady IR PL (which is proportional to $\eta_{TET} \times (power\ flux)$) for solution of TIPS-Tc (200 mg/mL) and PbS/TetCAL (1-100 mg/mL). The low and high triplet generation density, asymptotic forms for the triplet transfer efficiency (with slope 1 and 0.5) were overlaid for the case of 1 mg/mL of PbS/TetCAL. b) Predicted threshold intensities, G_{Th}, G_{α} and G_{beta}, as function of the PbS/TetCAL concentration ($\alpha = \beta = 0.95$). The equivalent solar flux available for absorption by TIPS-Tc under the AM1.5g spectrum (red horizontal dashed line). c) Simulation of the solution phase SF-PM efficiency normalised by the PbS/TetCAL QD intrinsic PLQE, under 532 nm excitation. Including the drop in PLQE due to photons absorbed directly to the PbS/TetCAL

QD. Two contours of interest are highlight; the region in which the PM efficiency is larger than the QD PL efficiency η_{QD} (black) and when PM efficiency is 95% of the upper limit for PM efficiency given by the singlet fission yield (purple line). The equivalent solar flux available for absorption by TIPS-Tc under the AM1.5g spectrum (red horizontal dashed line).

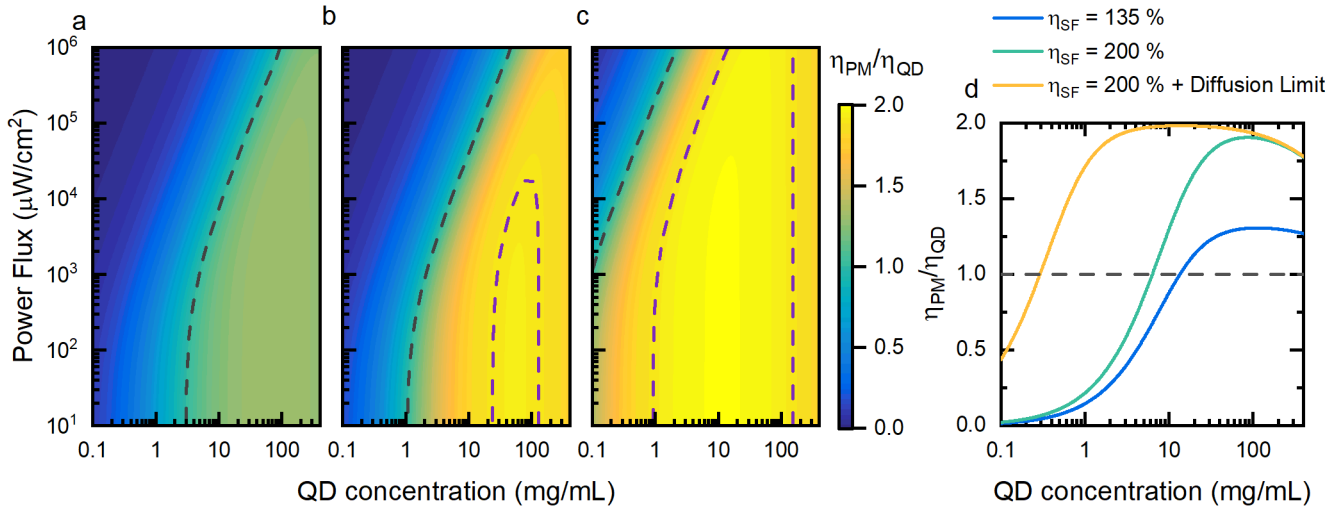

Figure S 29: Simulations of the SF-PM efficiency normalised by the PbS/TetCAL QD intrinsic PLQE, under 532 nm excitation. a) triplet kinetics and singlet fission yield (135%) as experientially observed. Prediction of the SF-PM efficiency for singlet fission yield of 200%, with the triplet kinetics as measured (b) and for triplet transfer at the expected diffusion limited rate (c). Points at which the normalised photon multiplication efficiency are unity (black dashed line) and 190% (purple dashed line). d) Simulated photon multiplication normalised efficiency at effective solar fluence (13.7 mW/cm²).

11 Steady State IR PL

We use PL/Power as a measure of relative PLQE. For the solutions with TIPS-Tc (200 mg/mL) and 2 mg/mL of PbS/TetCAL QDs, PL/Power drops off at a rate, with respect to the power flux, close to the predicted (Figure S30b). The relative IR PLQE for the solution with 100 mg/mL of PbS/TetCAL QDs is unchanged below the solar-equivilent fluence. However, the relative PLQE does start decreasing at lower powers than expected. The drop in PL for 100 mg/mL of dots at high power flux is larger than expected from the bi-molecular decay of the TIPS-Tc triplets. This could be an indication of photo bleaching of the TIPS-Tc or non-radiative decay in the QD.

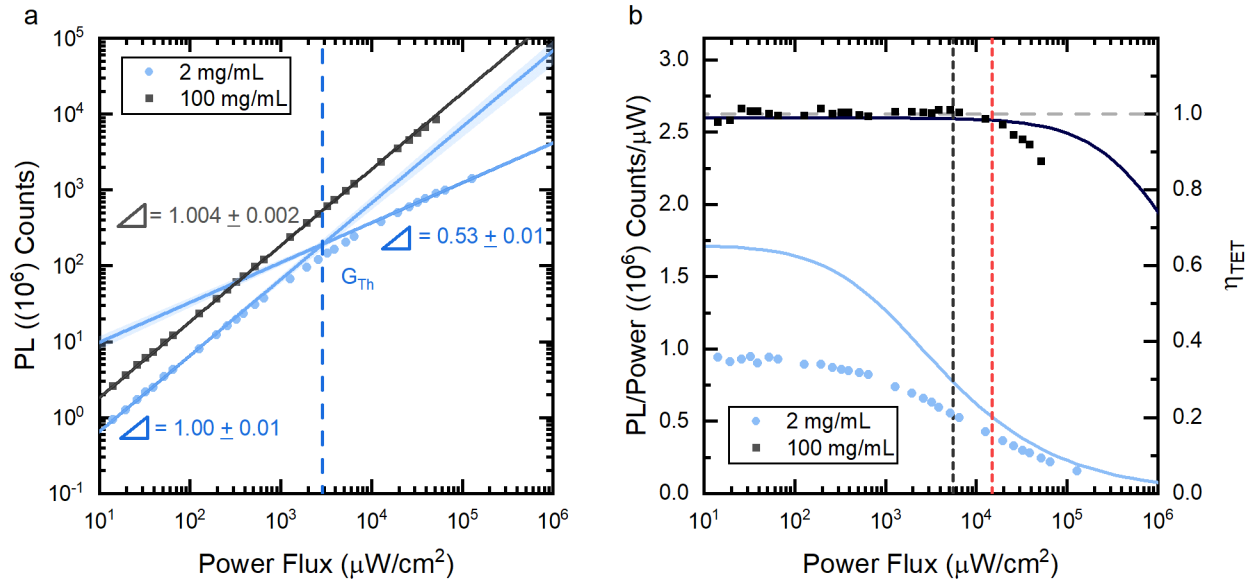

Figure S 30: a) Total IR PL counts from PbS/TetCAL QDs for solutions of low (2 mg/mL, blue circles) and high (100 mg/mL, black squares) QD concentration with TIPS-Tc (200 mg/mL) for varying 532 nm excitation flux. The PL counts were fit with power law relations to laser

flux, either across the entire flux range (100 mg/mL) or separated into two fits (2 mg/mL), for low and high photon flux. The intercept of the fits to the low and high flux regimes gives as 2.9 ± 1.0 mW/cm² as the threshold power flux (blue vertical dashed line). b) IR PL normalised by the incident power flux, giving the relative PL yield, as a function of the incident power flux (black and blue dots). Simulated triplet transfer efficiencies using the equations for the triplet transfer efficiency for 2 mg/mL (blue line) and 100 mg/mL (black line) PbS/TetCAL QD concentrations. The vertical dashed black line indicates the laser fluence used in the IR PLQE measurements (500 µW/cm²), while the red dashed line indicates the equivalent solar fluences (13.7 mW/cm²).

12 Magnetic Field Dependent PL

The TIPS-Tc singlet shows an increased PL on application of high magnetic fields (>0.3 T), as expected for a singlet undergoing are singlet fission (figure S31). While, the PbS/TetCAL IR PL shows a corresponding decrease, indicating that the excited QD states are the result of triplets generated by singlet fission, transferred from the TIPS-Tc.[4,15] Direct excitation of the PbS/TetCAL QD with 658 nm laser light results in no observed magnetic dependence (for fields less than 0.5 T), similar to previous observations.[4,15]

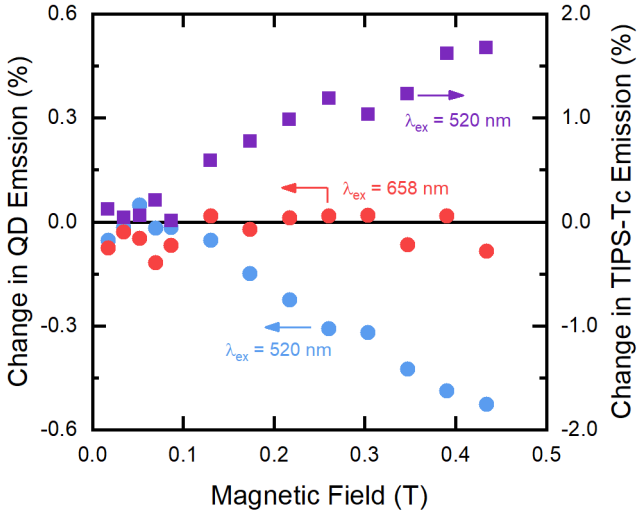

Figure S 31: Percentage change in the QD (red and blue circles) and TIPS-Tc (purple squares) PL, for solutions of TIPS-Tc (200 mg/mL) and PbS/TetCAL (100 mg/mL). QD emission resulting from triplet transfer from TIPS-Tc after excitation with 520 nm laser light (blue circles) drops on application of a high magnetic field (>0.3 T). Whereas, PL from the TIPS-Tc increases with large applied magnetic fields (purple squares). Direct excitation of the QD, with 658 nm laser light, results in no effect with applied magnetic field (red squares).

13 References

1. Garakyaraghi, S., Mongin, C., Granger, D. B., Anthony, J. E. & Castellano, F. N. Delayed Molecular Triplet Generation from Energized Lead Sulfide Quantum Dots. *J. Phys. Chem. Lett.* **8**, 1458–1463 (2017).
2. Hines, M. A. & Scholes, G. D. Colloidal PbS Nanocrystals with Size-Tunable Near-Infrared Emission: Observation of Post-Synthesis Self-Narrowing of the Particle Size Distribution. *Adv. Mater.* **15**, 1844–1849 (2003).
3. Mello, J. de, Wittmann, H. & Friend, R. An improved experimental determination of external photoluminescence quantum efficiency. *Adv. Mater.* **9**, 230–232 (1997).
4. Tabachnyk, M. *et al.* Resonant energy transfer of triplet excitons from pentacene to PbSe nanocrystals-Supplementary Information. *Nat. Mater.* **13**, 1033–1038 (2014).
5. Rao, A. *et al.* The role of spin in the kinetic control of recombination in organic photovoltaics. *Nature* **500**, 435–9 (2013).
6. Gelinas, S. *et al.* Ultrafast Long-Range Charge Separation in Organic Semiconductor Photovoltaic Diodes. *Science (80-.).* **343**, 512–516 (2014).
7. Zeng, B. *et al.* Characterization of the Ligand Capping of Hydrophobic CdSe–ZnS Quantum Dots Using NMR Spectroscopy. *Chem. Mater.* **30**, 225–238 (2018).
8. Hines, M. A. & Scholes, G. D. Colloidal PbS Nanocrystals with Size-Tunable Near-Infrared Emission: Observation of Post-Synthesis Self-Narrowing of the Particle Size Distribution. *Adv. Mater.* **15**, 1844–1849 (2003).
9. Davis, N. J. L. K. *et al.* Singlet Fission and Triplet Transfer to PbS Quantum Dots in TIPS-Tetracene Carboxylic Acid Ligands. *J. Phys. Chem. Lett.* **9**, 1454–1460 (2018).
10. Patnaik, P. *Handbook of inorganic chemicals*. (McGraw-Hill, 2003).
11. Moreels, I. *et al.* Size-dependent optical properties of colloidal PbS quantum dots. *ACS Nano* **3**, 3023–3030 (2009).
12. Futscher, M. H., Rao, A. & Ehrler, B. The Potential of Singlet Fission Photon Multipliers as an Alternative to Silicon-Based Tandem Solar Cells. *ACS Energy Lett* **22**, (2018).
13. Jafari, S. M., He, Y. & Bhandari, B. Production of sub-micron emulsions by ultrasound and microfluidization techniques. *J. Food Eng.* **82**, 478–488 (2007).
14. Patel, C. K. N. & Tam, A. C. Quantitative spectroscopy of micron-thick liquid films. *Appl. Phys. Lett.* **36**, 7–9 (1980).
15. Thompson, N. J. *et al.* Energy harvesting of non-emissive triplet excitons in tetracene by emissive PbS nanocrystals. *Nat. Mater.* **13**, 1039–1043 (2014).
16. Xu, S. *et al.* What is a convincing photoluminescence quantum yield of fluorescent nanocrystals. *J. Phys. Chem. C* **114**, 14319–14326 (2010).
17. Stern, H. L. *et al.* Identification of a triplet pair intermediate in singlet exciton fission in solution. *Proc. Natl. Acad. Sci.* **112**, 7656–7661 (2015).
18. Dover, C. B. *et al.* Endothermic singlet fission is hindered by excimer formation. *Nat. Chem.* **10**, 305–310 (2018).

19. Collins, F. C. & Kimball, G. E. Diffusion-Controlled Reactions in Liquid Solutions. *Ind. Eng. Chem.* **41**, 2551–2553 (1949).

20. Cheng, Y. Y. *et al.* Kinetic Analysis of Photochemical Upconversion by Triplet-Triplet Annihilation: Beyond Any Spin Statistical Limit. *J. Phys. Chem. Lett* **1**, 1795–1799 (2010).

21. NREL. Reference Air Mass 1.5 Spectra. Available at: https://www.nrel.gov/grid/solar-resource/spectra-am1.5.html. (Accessed: 5th June 2019)